UniTs - University of Trieste

Faculty of Scientific and Data Intensive Computing

Department of mathematics informatics and geosciences

Galaxy Astrophysics

Lecturer:
Prof. Girardi Marisa

Author:
Andrea Spinelli

November 30, 2025

github.com/Spina02 andreaspinelli2002@gmail.com

Preface

This course provides a comprehensive overview of galaxy astrophysics, structured as follows:

- **Fundamentals** (approximately 10 hours)
  - Stars
- **Phenomenology** (approximately 25 hours)
- **Dynamics of Non-collisional Systems**
  - Elliptical galaxies
  - Galaxy clusters

Reference Textbooks:

- **Introductory**
  - Karttunen et al., “Fundamental Astronomy”
  - Schneider, P. (2015), “Extragalactic Astronomy and Cosmology”
- **Advanced**
  - Binney, J. & Merrifield, M., “Galactic Astronomy”
  - Binney, J. & Tremaine, S., “Galactic Dynamics”

Contents

1 Introduction

When we observe the sky, we perceive it as a 2D surface, even though celestial objects actually exist in 3D space. To bridge this gap and measure distances in astronomy it is used a set of techniques known as the *distance ladder*. It consists of different methods, where each one relies on a specific physical phenomenon and is calibrated using the preceding method in the ladder. Only recently have precise instruments like ESA's Hipparcos (1989) and Gaia (2013) satellites enabled highly accurate stellar parallax measurements, with Gaia mapping distances to over a billion stars.

1.1 Reference Systems

To describe the position of an object in the sky, we need to define a reference system. For this purpose, astronomers often imagine all celestial objects as lying on a vast, imaginary *celestial sphere*, centered on the observer. Although this model has ancient origins, it remains extremely useful today. Since the celestial sphere is considered to have an infinite radius, we can ignore the small shifts caused by the Earth's rotation and orbit.

1.1.1 The Equatorial System

The **equatorial system** is defined by selecting a reference parallel and a reference meridian. The Earth's rotational axis remains nearly constant over time, so the equatorial plane (which is perpendicular to this axis) serves as a stable basis for a coordinate system that does not depend on the observer's location or the time of observation.

The ***celestial equator*** is the great circle where the celestial sphere meets the equatorial plane. The axis of this circle points toward the celestial poles. In the northern hemisphere, the north celestial pole is almost exactly aligned with the Earth's rotational axis and lies about one degree from Polaris.

The angle between a star and the celestial equator (the equatorial plane) remains unchanged by the Earth's daily rotation. This angle is called the ***declination*** δ ($-90^\circ < \delta < +90^\circ$). For the second coordinate, we also need a fixed direction that is independent of the Earth's rotation. This direction is defined by the *vernal equinox* (Υ), which is the point on the celestial sphere where the Sun's path (the ecliptic) crosses the celestial equator at the moment of the spring equinox. The second coordinate is then defined as the angle measured eastward along the celestial equator from the vernal equinox. This angle is called the ***right ascension*** α (or R.A.), with values ranging from 0 to 24 hours.

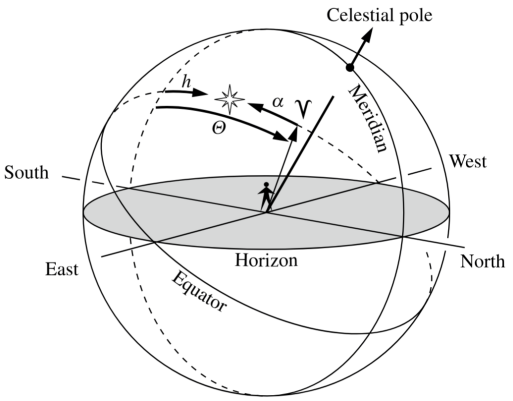

Figure 1.1: The Equatorial System [2]

The *sidereal time*, often denoted by Θ, measures the angle between the local meridian (The great circle on the celestial sphere that passes through both the celestial poles and the zenith of the observer) and the vernal equinox, increasing as the Earth rotates. For any celestial object, there is a simple and important relationship:

$$\Theta = h + \alpha$$

1.1.2 The Altazimuthal System or Horizontal System

The **azimuthal (or horizontal) system** is defined relative to the observer's specific position on Earth. Its reference plane is the local *horizon* (the plane tangent to the Earth at the observer's location). Where this plane meets the celestial sphere forms the visible horizon. The point directly overhead is the *zenith*; the point directly beneath is the *n*[illegible]

Great circles passing through the zenith are called *verticals*, and each one meets the horizon at a right angle. As the Earth rotates, stars appear to rise in the east, reach their highest point (culminate) when they cross the *meridian* (the vertical circle connecting north, zenith, and south) and set in the west. The intersection points of the meridian with the horizon define the north and south directions.

In this system, one coordinate is the ***altitude*** (or elevation), a, the angle between the horizon and the object along its vertical circle. Altitude ranges from $-90°$ to $+90°$, and is positive above the horizon.

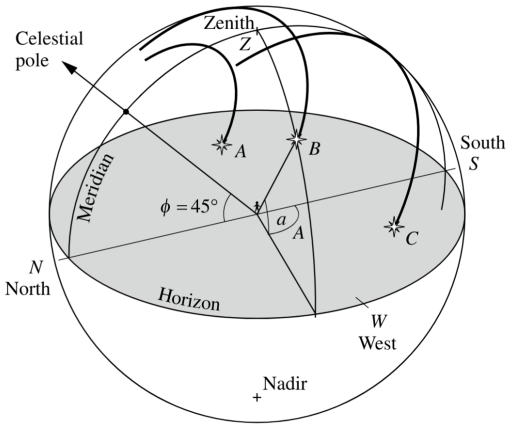

Figure 1.2: The Azimuthal System [2]

The second coordinate is the ***azimuth***, A: the angle measured along the horizon from a fixed reference direction to the object's vertical circle. The reference is often north or south, and by convention the angle is measured clockwise (see tip below).

Since this system depends on both the observer's position and the time, the coordinates of the same star will be different for different observers and at different moments. For this reason, horizontal coordinates are not used in star catalogues.

Tip: ***Azimuth direction***

There are different conventions for the reference direction and sense of azimuth, so it is always important to verify which one is being used. Here, we measure azimuth clockwise from the south, as is common in astronomy.

1.1.3 The Ecliptic System

The **ecliptic system** takes the Earth's orbital plane, the ***ecliptic***, as its fundamental reference. On the celestial sphere, the ecliptic is the great circle traced out by the Sun over the course of a year. This system is especially useful for mapping the positions of Solar System bodies.

The ecliptic and equatorial planes meet along the line pointing toward the *vernal equinox* (Υ), which serves as the zero point for both coordinate systems; at that moment, the Sun's coordinates are $\alpha = 0$ and $\delta = 0$. The two coordinates in this system are:

- The ***ecliptic latitude***, β, gives the angular distance from the ecliptic plane:
$$-90° \leq \beta \leq +90°$$
- The ***ecliptic longitude***, λ, measures the angle eastward (counterclockwise) from the vernal equinox:
$$0° \leq \lambda \leq 360°$$

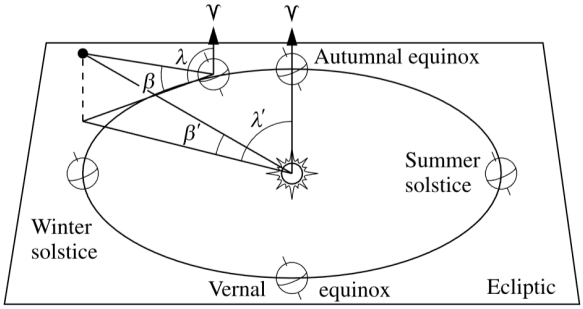

Figure 1.3: The Ecliptic System [2]

1.1.4 The Galactic System

For studies of the Milky Way Galaxy, the most natural reference plane is the plane of the Milky Way itself. Because the Sun lies very close to this plane, it is convenient to place the origin of the galactic coordinate system at the Sun.

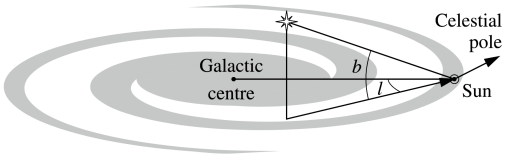

Figure 1.4: The Galactic System [2]

The ***galactic longitude*** l is measured counterclockwise (analogous to right ascension) along the galactic plane, starting from the direction of the center of the Milky Way, which lies in the constellation Sagittarius. The ***galactic latitude*** b is measured from the galactic plane: it is positive towards the north galactic pole and negative towards the south.

Observation: *Coordinate precision*

If right ascension is given in hours, we need to provide one additional decimal place in seconds compared to the declination, to preserve equivalent angular accuracy. For example:
$03^{h}\ 42^{m}\ 35.63^{s}$ $+42^{\circ}\ 32'\ 35.4''$

1.2 Coordinate perturbations

Even for a star fixed relative to the Sun, its observed coordinates may shift due to various perturbing effects. While altitude and azimuth change with Earth's rotation, even right ascension and declination are subject to small variations over time.

1.2.1 Precession and nutation

The Earth's rotational axis is not fixed in space; instead, it traces out a slow circular motion around the north pole of the ecliptic. This slow motion, known as ***precession***, causes the celestial poles and equator to shift over time, completing a full cycle roughly every 25,800 years. As a result, the coordinates of stars change slowly: star catalogues must specify the equinox, or reference epoch, to which their coordinates refer.

Superimposed upon precession is a smaller, periodic oscillation of the axis called ***nutation***. It is primarily caused by the gravitational pull of the Moon (and, to a lesser extent, the Sun) on Earth's equatorial bulge. This results in a short-term "nodding" motion, with the main period being about 18.6 years, as the Moon's orbital plane precesses.

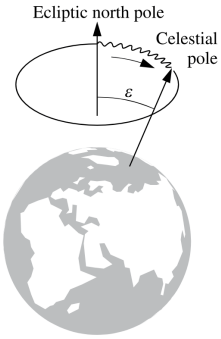

Figure 1.5: Precession and nutation [2]

Mathematically, the precessional motion can be described using the concept of torque:

$$\vec{\tau} = \frac{d\vec{L}}{dt}$$

where $\vec{L}$ is the angular momentum of the Earth, and $\vec{\tau}$ is the torque exerted mainly by the gravitational attraction of the Moon and Sun on the equatorial bulge. The change in angular momentum, $\Delta\vec{L}$, is perpendicular to $\vec{L}$, leading to a precession of the axis direction (rather than a change in tilt angle):

$$\Delta\vec{L} \perp \vec{L} \qquad \text{and} \qquad \vec{\tau} \perp \vec{L}$$

Both precession and nutation must be taken into account for precise astronomical coordinate systems, since they cause the celestial coordinate grid to shift over time.

Observation: *The vernal equinox point*

The vernal equinox point (♈) is not fixed in space. Due to the precession of Earth's axis, it gradually shifts westward along the ecliptic by approximately $50.25''$ (arcseconds) per year. This slow drift means that the celestial coordinate system itself must be periodically updated to a reference epoch in star catalogs and astronomical calculations.

1.2.2 Aberration

Since the Earth is moving, the direction to a star appears to be shifted by a small angle due to the Earth's velocity. This effect is called ***aberration***.

We can distinguish two types of aberration:

- **Annual aberration** is caused by the Earth's orbital motion around the Sun. This effect leads to a maximum apparent displacement of about $20.5''$ (arcseconds) in the direction of Earth's motion.
- **Diurnal (daily) aberration** is caused by the Earth's rotation about its axis. This produces a much smaller maximum displacement, about $0.32''$.

This phenomenon is usually already taken into account in the coordinates of the stars, so it is not necessary to correct for it.

1.2.3 Atmospheric refraction

Since light is refracted by the atmosphere, the direction of an object differs from the true direction by an amount depending on the atmospheric conditions along the line of sight.

If the object is not too far from the zenith, the atmosphere between the object and the observer can be approximated by a stack of parallel layers, each of which has a certain index of refraction n_i.

The zenith distance z of the object and the observed distance z_{obs} are related by the following equation:

$$n_0 \cdot \sin z_{obs} = n_1 \cdot \sin z_1 = \ldots = 1 \cdot \sin z$$

where n_i are the indices of refraction of the different layers.

Let $R = z - z_{obs}$ be the *refraction angle*. It holds that:

$$\begin{aligned} n_0 \cdot \sin z_{obs} &= \sin z = \sin(z_{obs} + R) \\ &= \underbrace{\sin R}_{\sim R} \cos z_{obs} + \underbrace{\cos R}_{\sim 1} \sin z_{obs} \\ \text{(for small } R\text{)} \quad &\approx \sin z_{obs} + R \cos z_{obs} \end{aligned}$$

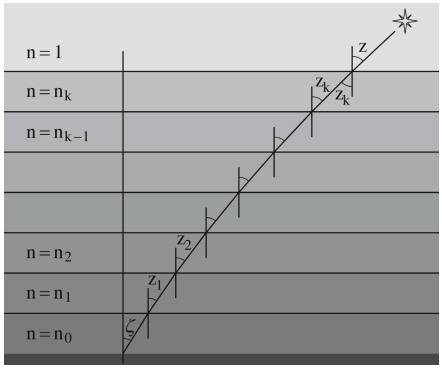

Figure 1.6: Refraction [2]

In addition to refraction, Earth's atmosphere also absorbs electromagnetic radiation, significantly impacting astronomical observations across various wavelengths:

- The **Troposphere** $(0 - 10\,\text{km})$, the lowest atmospheric layer, is composed primarily of H_2O, CO_2, CO, N_2, and O_2. These molecules here strongly absorb light in the **infrared (IR)** region.
- The **Stratosphere** $(10 - 80\,\text{km})$ contains a significant concentration of ozone (O_3), which efficiently absorbs light in both the **ultraviolet (UV)** and **X-ray** regions.
- The **Ionosphere** $(80 - 500\,\text{km})$ is a region rich in ionized particles; it absorbs **radio waves**.

Observation: *Absorption and observations*

The atmosphere blocks most IR, UV, and X-ray radiation, allowing only specific *windows* in the optical and radio. Thus, observations in these wavelengths must be done from space.

Beyond Earth's atmosphere, the **interstellar medium (ISM)**, composed of gas and dust, also absorbs and scatters electromagnetic radiation, particularly at **X-ray** and **UV** wavelengths.

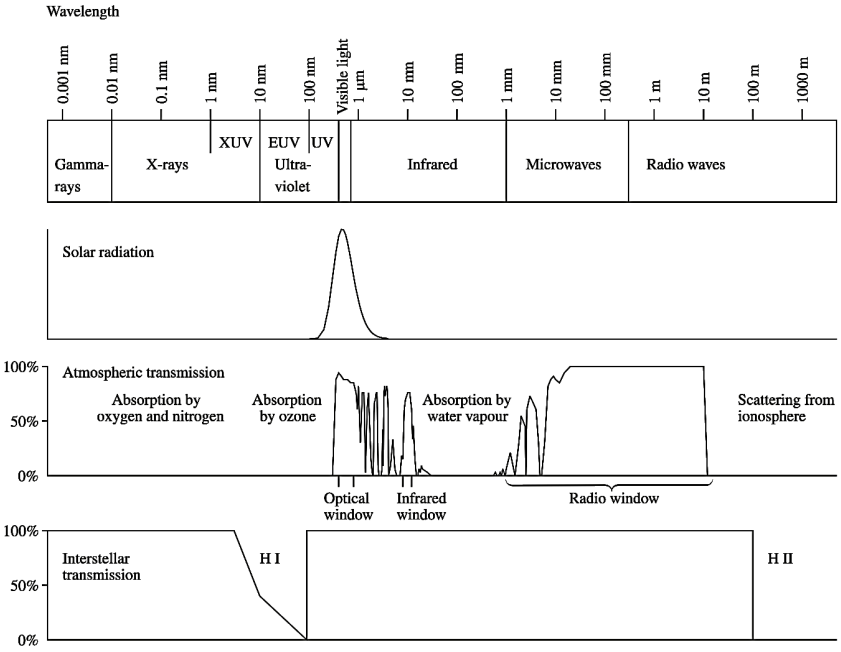

Figure 1.7: Atmospheric and interstellar absorption and transmission at different wavelengths: the top band shows the electromagnetic spectrum, followed by typical solar radiation at Earth; the third band displays atmospheric transmission with main absorption features (defining optical, infrared, and radio windows), while the bottom highlights interstellar absorption, especially by hydrogen, limiting UV and parts of the radio spectrum. [2]

Observation: *Zone of Avoidance*

The **Zone of Avoidance** is the region near the Galactic plane ($|\alpha| \lesssim 10°$) where absorption by dust and bright stars make optical observations of extragalactic objects very difficult.

1.2.4 Parallax

If we observe an object from different points, we see it in different directions. The difference of the observed directions is called the ***parallax***. The parallax effect highly depends on the distance of the object. The closer the object, the greater the parallax.

Since the Earth is moving, if an observer observes a star after an interval of time, he will be looking at the object from a different angle. We can distinguish two kinds of parallax:

- **Diurnal (daily) parallax** is due to the change of direction due to the daily rotation of the Earth. The diurnal parallax also depends on the latitude of the observer; if the position is not specified, it is assumed to be at the equator.
- **Annual parallax** is due to the Earth's orbital motion around the Sun. The annual parallax is the maximum parallax effect and it is used to measure the distance of the stars.

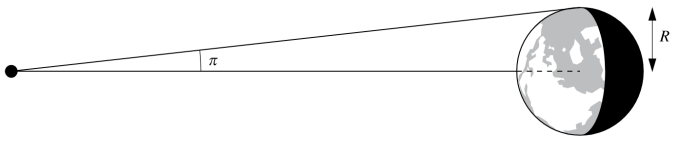

Figure 1.8: The parallax π is the angle subtended by the Earth's equatorial radius as seen from the object [2]

Astronomers typically express parallax angles in arcseconds for convenience. To convert a parallax measured in radians to arcseconds, we use the relation $\omega'' = 206265\,\omega$ [rad], where 206265 is the number of arcseconds in one radian.

Warning: *Parallax correction*

Usually, parallax correction is not taken into account in the coordinates of the star catalogues.

Over time, ”parallax” and ”distance” have practically become synonymous in astronomy, especially in the context of photometric parallax. In fact, it is the foundation for one of the most widely used units for astronomical distances: the parsec.

A **parsec** (pc) is defined as the distance at which an astronomical object would exhibit a parallax angle of $1''$ (one arcsecond), when measured from two points separated by 1 astronomical unit, that is, from opposite sides of Earth's orbit around the Sun six months apart.

Numerically, one parsec is approximately 3.26 light-years, or about 3.086×10^{16} meters.

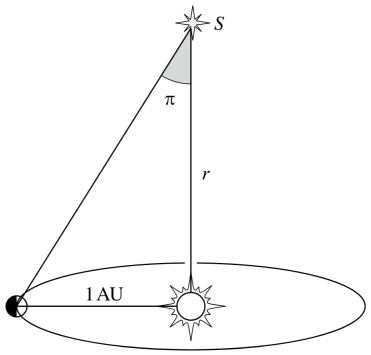

Figure 1.9: Parallax π of a star S is the angle subtended by the radius of the orbit of the Earth [2]

Over time, advancements in astronomical instrumentation have enabled increasingly precise measurements of stellar parallax, allowing us to probe greater distances:

Method/Instrument	Parallax Precision	Distance Limit
From Earth	$\pi \approx 0.01''$	up to ∼30 pc
Hipparcos satellite	$\pi \approx 0.001''$	up to ∼1000 pc
Gaia mission	$\pi \approx 2 \cdot 10^{-4}{}''$	up to ∼5000 pc (5 kpc)

Observation: ***Parallax measurement***

The objects with the largest measured parallaxes are some of the stars nearest to the Sun. Some notable examples include:

- In 1838, Bessel measured the parallax of 61 Cygni: $\pi = 0.29''$
- Proxima Centauri, the closest star to the Sun: $\pi = 0.75''$

1.2.5 Observations from Satellites

Observing from space-based telescopes and satellites provides several significant advantages over ground-based astronomical observations:

- **Absence of Atmospheric Refraction:** Earth's atmosphere bends and distorts incoming starlight; outside the atmosphere, these effects are avoided, resulting in more reliable measurements.
- **No Gravitational Flexure:** In orbit, instruments are effectively weightless, removing distortions caused by gravitational sagging that affect even the best ground-based observatories.
- **Sharper Images:** Space telescopes are unaffected by atmospheric blurring, so resolution is limited only by their optics (Airy disk), not by seeing.
- **Stable Observational Conditions:** Space offers a stable thermal and radiation environment, allowing for superb calibration and highly repeatable measurements across long timescales.

As a result, satellite missions such as *Hipparcos* and *Gaia* have revolutionized parallax measurements with unprecedented accuracy and reach.

Furthermore, since a star's observed flux (F) diminishes with the square of its distance (d) from us ($F \propto d^{-2}$), uncertainties in distance measurements are amplified in the derived fluxes. If the fractional uncertainty in distance is $\frac{\Delta d}{d}$, then the corresponding fractional uncertainty in the flux is:

$$\frac{\Delta F}{F} \approx 2 \cdot \frac{\Delta d}{d}$$

E.g., if the parallax-based distance has a relative uncertainty of 20% ($\frac{\Delta d}{d} \sim 0.2$), the resulting uncertainty in the flux is $\frac{\Delta F}{F} \sim 40\%$, underlining the importance of minimizing distance errors.

1.3 Positional Astronomy

Any space motion can be decomposed into two components: the ***radial velocity*** (line-of-sight, LOS, v_r), directed along the observer's line of sight, and the ***tangential velocity*** (v_t), perpendicular to it.

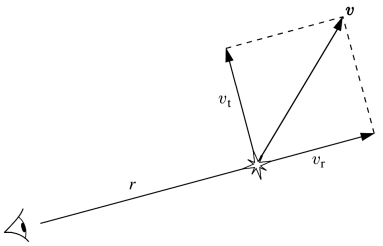

$$v = \sqrt{{v_t}^2 + {v_r}^2}$$

As the universe is expanding, many extragalactic objects are moving away from us, and their light is observed to be shifted towards longer (redder) wavelengths. This is known as the ***redshift*** (z). This phenomenon is fundamentally similar to the Doppler effect for sound.

To understand the shift in wavelength, consider a source emitting electromagnetic waves with period T. If the source were at rest with respect to the observer, the emitted wavelength would be:

$$\lambda_0 = cT$$

where c is the speed of light.

If the source moves at velocity v relative to the observer (positive when receding, negative when approaching), during the same period T it covers a distance $s' = vT$ relative to the observer.

Thus, the observed wavelength λ becomes:

$$\lambda = s + s' = cT + vT = (c+v)T$$

The change in wavelength is given by:

$$\Delta\lambda = \lambda - \lambda_0 = (c+v)T - cT = vT$$

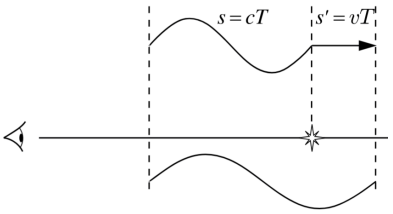

Figure 1.10: Wavelength shift [2]

1.3.1 Redshift

We define the ***redshift*** z as the fractional change:

$$z = \frac{\Delta\lambda}{\lambda_0} = \frac{vT}{cT} = \frac{v}{c}$$

This result applies when $v \ll c$ (non-relativistic limit).

For high velocities (e.g., distant galaxies or quasars), use the relativistic expression:

$$z = \sqrt{\frac{1+\frac{v}{c}}{1-\frac{v}{c}}} - 1$$

which for $v \ll c$ reduces to the previous, linear relation. In most stellar and galactic contexts, velocities are much smaller than the speed of light ($v_{stars} = 2-400\,\mathrm{km/s}$, $v_{galaxies} \sim 10^3\,\mathrm{km/s}$, while $c = 3\cdot 10^5\,\mathrm{km/s}$), so the non-relativistic approximation is sufficient.

An observed redshift generally has two main contributions: a ***kinematic*** term z_{kin} from the galaxy's peculiar motion and a ***cosmological*** term z_{cosm} from the expansion; they do **not** add linearly.

In a cluster of N galaxies, individual galaxies show slightly different observed redshifts z_i from both peculiar motions and expansion. The mean over N members defines the cluster redshift:

$$z_{\mathrm{cluster}} = \frac{1}{N}\sum_{i=1}^{N} z_i$$

Since peculiar velocities roughly average to zero in the cluster frame, this identifies the cosmological redshift:

$$z_{\text{cluster}} = z_{\text{cosm}}$$

For each galaxy in the cluster, we can define its "rest-frame" (or peculiar) redshift:

$$z_{\text{rf}} = \frac{z_{\text{obs}} - z_{\text{cluster}}}{1 + z_{\text{cluster}}}$$

Here, z_{obs} is the total observed redshift for an individual galaxy, z_{cluster} is the cosmological redshift of the cluster, and z_{rf} quantifies the galaxy's motion relative to the cluster frame.

1.3.2 Proper motion

Proper motion (μ) is a star's apparent angular motion across the sky relative to the Sun, measured in arcseconds per year. This motion is most evident for nearby stars or those with large *peculiar motions* (different from the Sun's motion).
A star's space velocity splits into a ***radial velocity*** (v_r) and a ***tangential velocity*** (v_t). The tangential velocity results in the proper motion, which can be measured by taking plates at intervals of several years or decades.

$$\tan\frac{\alpha}{2} \sim \frac{x/2}{d} \qquad \Rightarrow \qquad \mu \sim \frac{v_t}{d}$$

Thus, the tangential velocity follows from the proper motion and the distance:

$$v_t = 4.74\,\mu\,d$$

where 4.74 converts to km/s when using the units below:

$$[v_t] = \text{km/s} \qquad [d] = \text{pc} \qquad [\mu] = \text{arcsec/year}$$

The proper motion μ is usually described in terms of two components: one along the declination direction, $\mu_\delta = \Delta\delta\,/\,1\,\text{year}$, and one along the right ascension direction.

However, to properly express the motion in right ascension, we need to take into account that lines of right ascension (hour circles) get closer together as you move away from the celestial equator towards the poles. Therefore, the component in right ascension is written as $\mu_\alpha^* = \mu_\alpha \cos\delta$, with $\mu_\alpha = \Delta\alpha\,/\,1\,\text{year}$, where the factor of $\cos\delta$ adjusts for this effect.
The total proper motion is then:

$$\mu = \sqrt{\mu_\delta^2 + \mu_\alpha^2 \cos^2\delta} \qquad \text{or} \qquad \mu = \sqrt{\mu_\delta^2 + (\mu_\alpha^*)^2}$$

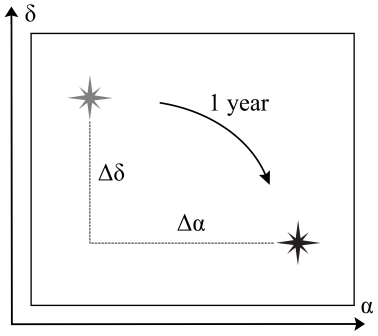

Figure 1.11: Proper motion [2]

Observation: ***Barnard's Star***

Barnard's Star exhibits the highest known proper motion of any star, moving across the sky at a remarkable rate of $\mu = 10.34$ arcsec/year.

1.4 Magnitudes

1.4.1 Intensity, Flux Density and Luminosity

Photometry quantifies how bright an object appears by connecting physical quantities such as specific intensity, flux and luminosity with the logarithmic magnitude scale used in astronomy.

Consider the energy from radiation passing through a surface element dA. Let this energy propagate into a solid angle $d\omega$ at an angle θ to the surface normal. The amount of ***energy*** within the frequency range $[\nu, \nu + d\nu]$ that passes into this solid angle in a time interval dt is:

$$dE_\nu = I_\nu \cos\theta \; dA \; d\nu \; d\omega \; dt$$

Here, the coefficient I_ν is the ***specific intensity of the radiation*** at the frequency ν in the direction of the solid angle $d\omega$.

In other words, the specific intensity is the amount of energy passing through a surface element in a given direction, per unit area, per unit time, per unit frequency and per unit solid angle:

$$[I_\nu] = \mathrm{W m^{-2} Hz^{-1} Sterad^{-1}}$$

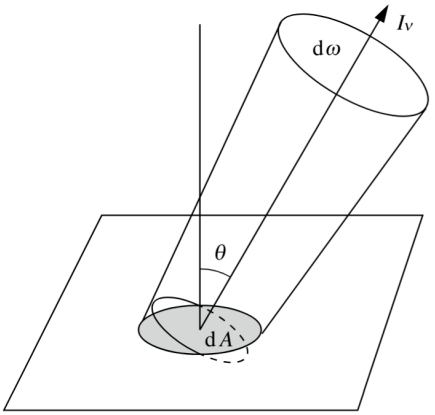

Figure 1.12: I_ν is the energy through dA into $d\omega$, direction θ [2]

The **Surface Brightness** (SB) is used to describe the brightness of an extended object in the sky:

$$SB = \frac{Flux}{Solid\ Angle}$$

The **total intensity** I is obtained by integrating I_ν over all frequencies:

$$I = \int_0^\infty I_\nu d\nu$$

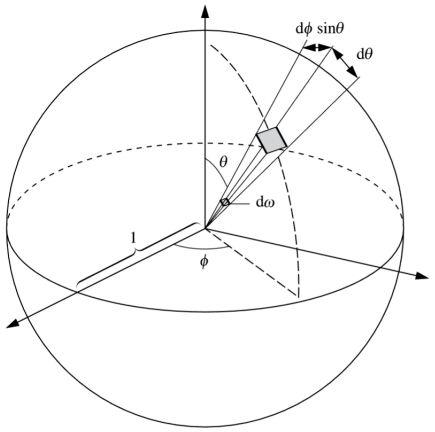

Figure 1.13: Solid angle $d\omega$ [2]

From an observational standpoint, a more practical quantity is the **flux density**, often simply called ***flux***, which represents the power of radiation received per unit area. The monochromatic flux density F_ν is the energy passing through a surface element per unit area, per unit time, and per unit frequency:

$$F_\nu = \frac{1}{dA\, d\nu\, dt} \int_S dE_\nu = \int_S I_\nu \cos\theta \, d\omega, \qquad [F_\nu] = \mathrm{W\, m^{-2} Hz^{-1}}$$

Analogously, the **total flux** F is obtained by integrating over all frequencies:

$$F = \int_0^\infty F_\nu d\nu = \int_S I \cos\theta \, d\omega, \qquad [F] = \mathrm{W\, m^{-2}}$$

Observed flux densities are usually very small, so a more convenient unit is often used, particularly in radio astronomy: the ***Jansky*** (Jy), defined as: $1\mathrm{Jy} = 10^{-26} \mathrm{W\, m^{-2} Hz^{-1}}$.

The ***luminosity*** L of an object is the power emitted by the object throughout a closed surface surrounding it, and it is given by:

$$L = \int_{\Sigma} F \, dA$$

For a spherically symmetric source radiating into a solid angle ω, the flux measured at distance r is related to luminosity by

$$L = \omega r^2 F,$$

In the most common case of isotropic emission ($\omega = 4\pi$), this reduces to

$$L = 4\pi r^2 F.$$

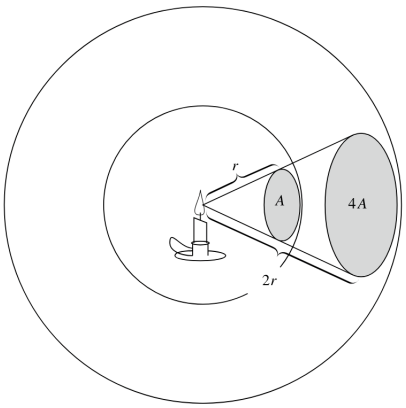

Figure 1.14: Luminosity [2]

Observation: ***Inverse square law***

Unlike the surface brightness, the observed flux from a source decreases as the square of the distance from the observer, this is known as the **inverse square law**:

$$F = \frac{L}{4\pi r^2} \propto \frac{1}{r^2}$$

The SI unit of luminosity is the watt (W), where $1\ \mathrm{W} = 1\ \mathrm{J\,s^{-1}}$. Astronomers often compare stellar luminosity to the solar luminosity, $L_\odot \approx 3.828 \times 10^{26}$ W.

1.4.2 Apparent Magnitude

Historically, stellar brightness was estimated by eye into a few *magnitude classes*: the brightest stars were called first magnitude and the faintest visible to the naked eye sixth magnitude. In modern usage, the **apparent magnitude** of a source is defined by

$$m = -2.5 \log_{10}\left(\frac{f}{f_0}\right)$$

where f is the measured flux in a given photometric band and f_0 is the corresponding *reference flux*. In the **Vega system**, f_0 is the flux of Vega in that band, so Vega is defined to have $m = 0$. A widely used alternative is the **AB system**, in which the zero point corresponds to a constant specific flux density of 3631 Jy (i.e. $\approx 3.63 \times 10^{-20}\ \mathrm{erg\,s^{-1}\,cm^{-2}\,Hz^{-1}}$) for all bands; in this system Vega is not the reference. Furthermore, for the AB system, the zero point is defined such that $V_{\mathrm{AB}} = V_{\mathrm{vega}}$ for the V band (to within a small offset).

More generally, the difference in apparent magnitude between two sources with fluxes f_1 and f_2 (magnitudes m_1 and m_2) is given by the ***Pogson relation***:

$$m_1 - m_2 = -2.5 \log_{10}\left(\frac{f_1}{f_2}\right)$$

so an increase of five magnitudes corresponds to a factor of 100 decrease in flux (one magnitude corresponds to a factor of $10^{0.4} \approx 2.512$).

Equivalently, the flux ratio can be written as

$$\frac{f_1}{f_2} = 10^{-0.4\,(m_1 - m_2)}$$

Spectral Energy Distribution

The flux we detect from an astronomical source is spread over a range of energies or wavelengths. The **spectral energy distribution** (SED) describes the flux density as a function of either frequency, f_ν (measured in $\mathrm{W\,m^{-2}\,Hz^{-1}}$), or wavelength, f_λ (measured in $\mathrm{W\,m^{-2}\,nm^{-1}}$). The SED encodes important physical information about the source, such as its temperature, composition, and emission mechanisms.

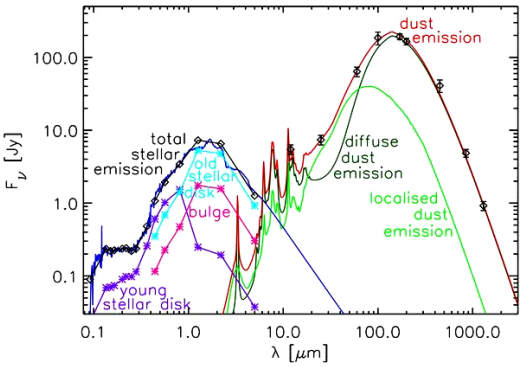

Why do we use the apparent magnitude?

It is not always possible to measure the monochromatic flux of a source directly, because the detected signal is modified by the atmosphere, filters and the telescope+detector response. In a given photometric band, the measured flux f is the source spectral energy distribution f_ν weighted by the total system throughput:

$$f = \int_0^\infty f_\nu T_\nu F_\nu R_\nu \, d\nu$$

where f_ν is the flux density from the source above the atmosphere. The other factors describe the response of each element in the optical path:

- **Atmospheric transmission** T_ν:
  Quantifies how the atmosphere absorbs and scatters incoming light before it reaches the ground.

  The transmission decreases exponentially with increasing airmass a (the path length through the atmosphere), following $T_\nu = e^{-\tau_\nu a}$, where τ_ν is the optical depth at frequency ν. The airmass is given by $a = \frac{1}{\cos(z)}$, with z the zenith angle.

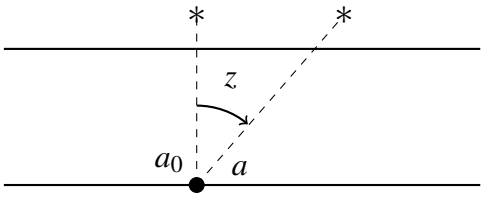

  Atmospheric extinction consists of both absorption and scattering by molecules and aerosols. It increases with airmass and is typically parameterized using a linear relation in magnitudes:

$$m(z) = m_0 + ka$$

  where $m(z)$ is the observed magnitude at zenith angle z, m_0 is the magnitude outside the atmosphere (zero airmass), k is the extinction coefficient (which depends on wavelength and atmospheric conditions), and a is the airmass, given by $a = 1/\cos(z)$. Alternatively, the airmass can also be expressed as $a = \alpha x$ for more precise geometric corrections, with α a proportionality constant and x a path-length factor.

  An important process in atmospheric extinction is **Rayleigh scattering**: the scattering of light by small molecules. Rayleigh scattering is much stronger at shorter wavelengths (blue light), making the sky blue and causing stronger extinction for bluer astronomical sources.

- **Filter response** F_ν:
  Describes the transmission curve of the photometric filter, which determines how efficiently the filter transmits light at each frequency or wavelength. The effective bandpass and central wavelength are defined by this curve.

In practice, we often use the **effective (mean) wavelength**, defined as:

$$\lambda_{\text{eq}} = \frac{\int \lambda\, T_\lambda\, F_\lambda\, R_\lambda\, d\lambda}{\int T_\lambda\, F_\lambda\, R_\lambda\, d\lambda}$$

where the integrals are performed over the bandpass and T_λ, F_λ, R_λ are the atmospheric, filter, and detector response curves, respectively. The full width at half maximum (FWHM) is often used to characterize the width of the filter's transmission profile.

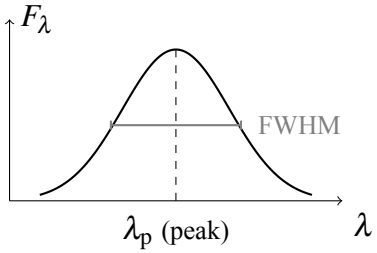

Figure 1.15: Profile of a photometric filter response.

- **Telescope and detector response** R_ν:
  Represents the overall efficiency of the instrument, including the optics, mirrors, and detector (such as a CCD), and accounts for the quantum efficiency and reflective losses at each stage. Accurate knowledge of R_ν is essential for reliable photometry.
  - **Photographic plates**: Early photographic plates had relatively poor photometric accuracy, with typical uncertainties around $\Delta m \approx 0.03$ mag.
  - **CCD (Charge-Coupled Devices)**: Modern CCDs revolutionized photometry, offering uncertainties as low as $\Delta m \approx 0.001$ mag thanks to high quantum efficiency and linear response.
  - **Photoelectric photometry**: Also widely used, providing precise measurements of incident flux using the photoelectric effect.

Observation: ***K-correction***

For galaxies at significant cosmological distances, one must apply a *K-correction* to account for the fact that their observed light is redshifted due to cosmic expansion.

1.4.3 Absolute Magnitude

The **absolute magnitude** M of an astronomical object measures how bright it would appear if it were placed at a distance of 10 parsecs, removing the effects of distance to reflect its true luminosity. More formally, the relationship between apparent magnitude m, absolute magnitude M, and distance d (in parsecs) is governed by the distance modulus formula:

$$m - M = -2.5 \log\left(\frac{f}{F}\right)$$

Here, f is the observed flux received from the source at an arbitrary distance d, and F is the flux the same source would produce at exactly 10 pc. Since flux decreases with the square of the distance, this relation naturally encodes the effects of distance on observed brightness.

Knowing the relationship between flux and distance, we can derive the following relations:

$$m - M = 5\log_{10}(d) - 5$$

$$m = M + 5\log_{10}(d) - 5$$

$$M = m - 5\log_{10}(d) + 5$$

The term $m - M$ is called the ***distance modulus***. It provides a convenient tool for determining absolute magnitude when both apparent magnitude and distance are measured, and vice versa.

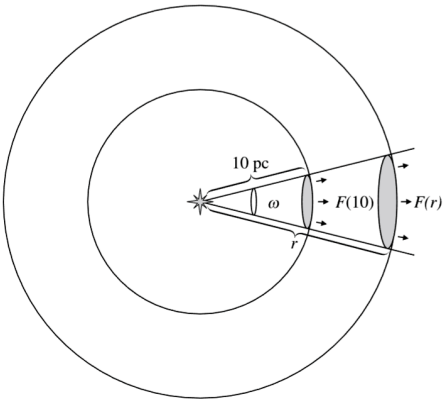

Figure 1.16: Absolute magnitude [2]

Observation: *Absolute Magnitude of the Sun*

The **absolute magnitude** of the Sun in the V band is $M_{V\odot} = 4.83$.
The apparent V-band magnitude of the Sun as observed from Earth is $V_\odot = -26.74$. The **distance modulus** for the Sun is:

$$(V - M_V)_\odot = V_\odot - M_{V\odot} = -26.74 - 4.83 = -31.57$$

1.4.4 Color Index

To measure stellar magnitudes with the highest precision, astronomers rely on photoelectric photometers, combined with carefully selected filters that restrict the incoming light to a specific wavelength range. The most widely adopted system is the *Johnson photometric system*, which originally used three principal filters: U (ultraviolet), B (blue), and V (visual).
The initial UBV system was later extended to the UBVRI, including R (red) and I (infrared). Each filter samples a distinct portion of the object's SED, so by comparing magnitudes measured through different filters, we gain direct information about a source's color and temperature.

In any photometric system, the difference between two magnitudes measured in different passbands is called a **color index**. For example, the $B-V$ color index is defined as:

$$B - V = m_B - m_V$$

where m_B and m_V are the magnitudes measured through the B and V filters.
More generally, the color index quantifies how the observed energy output changes between two wavelength intervals set by the respective filters. Formally, the $B-V$ color can be expressed as:

$$B - V = C - 2.5 \log \left(\frac{\int_0^\infty d\lambda \, \delta_\lambda(B) f_\lambda}{\int_0^\infty d\lambda \, \delta_\lambda(V) f_\lambda} \right)$$

where $\delta_\lambda(B)$ and $\delta_\lambda(V)$ are the response functions of the B and V filters, f_λ is the spectral flux density, and C is a system-dependent constant that ensures the correct photometric zero-point.
Importantly, the color index is independent of the source's distance:

$$B - V = M_B - M_V + \cancel{5 \log d} - \cancel{5} - \cancel{5 \log d} + \cancel{5} = M_B - M_V$$

where M_B and M_V are the absolute magnitudes in the B and V bands, respectively. The distance-dependent terms cancel, so the observed color index directly reflects intrinsic properties.

Building upon this, the color index emerges as a fundamental tool for probing the physical properties of stars and galaxies, such as temperature, age and stellar population types.

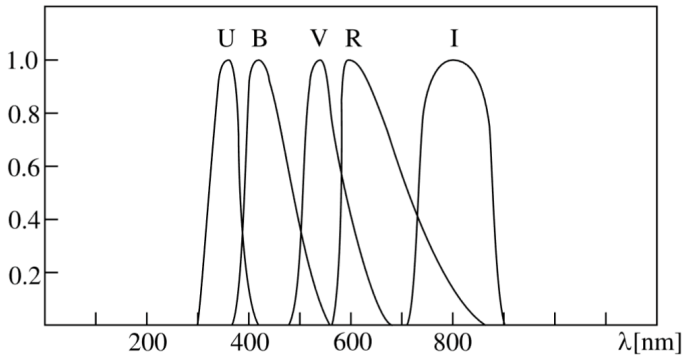

Figure 1.17: Relative transmission profiles of filters used in the UBVRI magnitude system. The maxima of the bands are normalized to unity. The R and I bands are based on the system of Johnson, Cousins, and Glass, which includes also infrared bands J, H, K, L, and M. Previously used R and I bands differ considerably from these. [2]

In particular, the $B-V$ color index serves as a straightforward and powerful temperature diagnostic for stars. Since hotter stars emit more radiation at shorter (bluer) wavelengths, they have lower (more negative) $B-V$ values; conversely, cooler stars appear redder and have higher $B-V$. The temperature corresponding to the color index is called **color temperature** T_c.
Color indices are also a useful diagnostic for broadly classifying the morphological types of galaxies. Elliptical galaxies typically exhibit redder colors, with $(B-V) \approx 1.5$, whereas spiral galaxies are generally bluer, around $(B-V) \approx 1.0$.

Tip: ***Practical use of color indices***

In practical terms, color indices such as $U-B$ and $B-V$ are commonly reported, while the V magnitude typically serves as the reference for absolute brightness.

1.4.5 Magnitude corrections

Magnitude corrections for stars

Interstellar dust and gas, collectively known as the Interstellar Medium (ISM), absorb and scatter starlight as it travels toward us. This process, called **interstellar extinction**, dims and reddens the observed light, causing the apparent magnitude m to differ from the star's intrinsic magnitude M.
To correct for interstellar extinction, astronomers rely on ***standard stars***: stars whose intrinsic magnitudes and colors are well known. By comparing the observed magnitudes of other stars to these calibrated standards, the effects of extinction can be accurately measured and removed.
To correct for extinction, we introduce the extinction term A_λ at wavelength λ:

$$M = m - 5\log(d) + 5 - A_\lambda$$

The value A_λ quantifies the amount of extinction suffered by the light at wavelength λ. It is stronger at shorter wavelengths due to the wavelength dependence of the ISM opacity, meaning that blue light is affected more than red. Specifically, as we move from blue to infrared filters we have: $A_B > A_V > A_R > A_I$. This differential extinction alters the observed color index. For the $(B-V)$ color, the correction is:

$$(B-V) = (B-V)_0 + \underbrace{A_B - A_V}_{E_{B-V} \neq 0}$$

where $(B-V)_0$ is the intrinsic (unreddened) color index and $E_{B-V} = A_B - A_V$ is the **color excess**. The color excess encapsulates how much the ISM has reddened the starlight.
The relationship between extinction and color excess is characterized by the ratio

$$R = \frac{A_V}{E_{B-V}} \approx 3$$

for the diffuse Milky Way ISM. R depends on properties, such as opacity, of the ISM along the line of sight. It is also related to the distance d travelled through the ISM:

$$A_V \propto d$$

Observation: ***Colour as a distance tracer***

By comparing a star's observed color to its intrinsic color $(B-V)_0$, if the stellar type is known, one can infer the color excess E_{B-V}, and thus estimate the extinction and, ultimately, the distance to the star.

Magnitude corrections for galaxies

To accurately determine the intrinsic brightness of galaxies, astronomers must account for several corrections that affect the observed magnitude. The full correction formula is:

$$M = m - 5\log(d) + 5 - A_\lambda - A_{\lambda,i} - K + E$$

where A_λ is the MW extinction, $A_{\lambda,i}$ is the intrinsic extinction of the galaxy (due to its ISM), K is the K-correction and E is the evolution correction.

It is important to note that elliptical galaxies exhibit minimal extinction because they contain very little interstellar dust and gas. In contrast, spiral galaxies often display significant extinction, especially when observed *"edge-on"* (when the disk of the galaxy is parallel to our line of sight) where starlight traverses a longer path through the galaxy's dusty disk.

- **K-correction**:
  The **K-correction** adjusts for the fact that, due to redshift, a galaxy's observed spectrum is shifted and stretched to longer wavelengths compared to its rest-frame spectrum. This means an observed filter samples bluer rest-frame light. To compare intrinsic properties of galaxies at different redshifts, this effect must be corrected. Wavelengths are related by:

  $$\lambda_{\text{obs}} = \lambda_{\text{RF}}(1+z)$$

  and thus, a filter of width $\Delta\lambda_{\text{obs}}$ corresponds to a narrower interval in the rest-frame:

  $$\Delta\lambda_{\text{RF}} = \frac{\Delta\lambda_{\text{obs}}}{1+z}$$

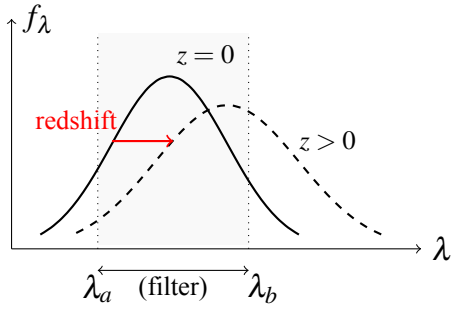

Figure 1.18: Effect of redshift on an observed galaxy spectrum: the rest-frame SED $z = 0$ is not only shifted towards longer wavelengths at $z > 0$ but also stretched (broadened) in wavelength. The features in the SED appear at longer wavelengths and are spread out due to the cosmological expansion. Thus, the fixed observed filter (between λ_a and λ_b) samples different and broader parts of the SED as redshift increases.

- **Evolution correction**:
  The **evolution correction** (E) accounts for changes in a galaxy's stellar population and luminosity over time. As galaxies age, their stars evolve, altering overall brightness and color. Thus, a galaxy seen at higher redshift (when the Universe was younger) may look intrinsically brighter or bluer, not due to distance or observational effects.
  - For **spiral galaxies**, we typically assume their star formation rate remains constant over time. The intrinsic properties of spirals change little, so the evolution correction is negligible:

    $$E \approx 0$$

  - In contrast, **elliptical galaxies** experienced most of their star formation in a brief, intense burst early in their history. Afterward, star formation largely ceased, and the stars passively age and redden. This causes their luminosity to fade significantly as the galaxy evolves. For these galaxies, the evolution correction can be substantial and is often parametrized as:

    $$E \sim K$$

    meaning that both evolutionary and K-corrections can be of similar magnitude and must be carefully accounted for when studying distant ellipticals.

- **Extinction**:
  We have already discussed extinction in the context of stars, and the same principles apply to galaxies as well. If there is no material absorbing light along the line of sight, the relation between luminosity and distance is simply given by $L = \omega r^2 F$, where L is the luminosity, F is the observed flux, ω is a geometric factor, and r is the distance to the source.
  However, when extinction occurs, the loss of light as it passes through the interstellar medium can be described by the equation

$$dL = -\alpha L dr$$

  where the parameter α, known as the ***opacity***, quantifies how effectively the medium absorbs or blocks the radiation.The effect of extinction on observed luminosity is conveniently described by the **optical thickness** τ, defined as:

$$d\tau = \alpha\, dr$$

  The change in luminosity is then:

$$dL = -L d\tau \qquad \Rightarrow \qquad \int_{L_0}^{L} \frac{dL'}{L'} = -\int_0^{\tau} d\tau' \qquad \Rightarrow \qquad L = L_0\, e^{-\tau}$$

  where L_0 is the intrinsic (unextinguished) luminosity.

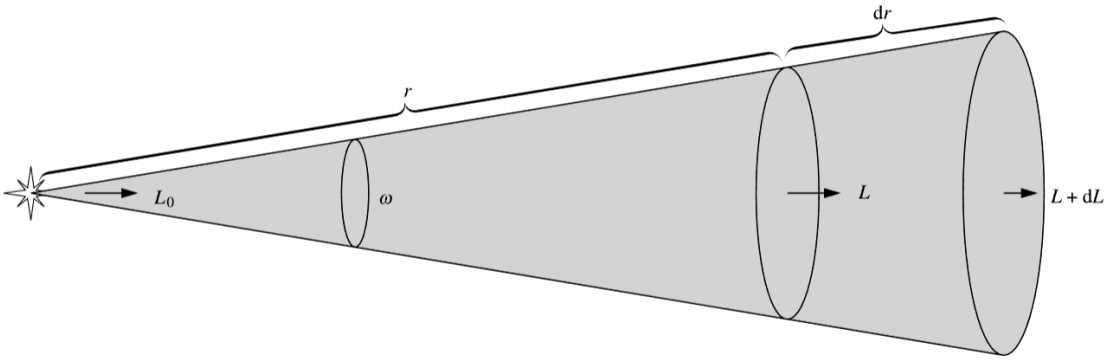

Figure 1.19: Extinction effect on the observed flux of a galaxy. [2]

  The effect of extinction on luminosity and flux can be written explicitly as:

$$L(r) = \omega r^2 F(r)$$

  where $L(r)$ is the luminosity at distance r, ω is a geometric factor, and $F(r)$ is the observed flux at r. Taking extinction into account, the observed flux becomes:

$$F(r) = F_0 \frac{R^2}{r^2} e^{-\tau}$$

  where F_0 is the flux at a reference distance (or from a standard star), R is the reference distance, and τ is the optical thickness (i.e., the total extinction along the line of sight).
  The distance modulus including extinction then becomes:

$$m - M = -2.5 \log\left(\frac{F(r)}{F(10\,\mathrm{pc})}\right)$$

  Substituting the expression for $F(r)$ and $F(10\,\mathrm{pc})$, we obtain:

$$m - M = 5 \log\left(\frac{r}{10\,\mathrm{pc}}\right) + \underbrace{2.5\,(\log e)\,\tau}_{A}$$

  where A is the total extinction in magnitudes ($A = 1.086\,\tau$).

1.4.6 Absolute Energy Distribution

2
Raw notes (To be rewritten)

MISSING: Lecture 21/10/2025

3 Lecture 23/10/2025

MISSING: Start of the lecture

3.1 Spiral Galaxies

	S_a	S_b	S_c	S_d
M_B	$-17-23$	$-17-23$	$-16-22$	$-15-20$
$M/M_\odot$	10^{9-12}	10^{9-12}	10^{9-12}	10^{8-10}
V_{max}	$163-367$	$163-367$	$99-304$	$99-304$
L_{bulge}/L_{tot}	0.3	0.13	0.05	?
$B-V$	0.75	0.64	0.52	0.47
M_{gas}/M_B	0.04	0.08	0.16	0.25

Another important parameter is the **Opening angle** θ_0, which is the angle between the major axis of the galaxy and the line of sight.
We can distinguish "grand design" and "flocculent" galaxies.

Surface	brightness	profile	M/L
Bulge	$2^{1/4}$	low	$\sim 5\frac{M_d}{L_\odot}$
Disk	expo	low	$\sim 3\frac{M_\odot}{L_\odot}$

There exists "Bulges" and "Pseudobulges".
We know very few pseudobulges.
Bulges have law of E
Pseudobulges have exopnential profile -> rotation
Freeman Law:
$\mu_0 \sim const$

$$\mu_0 = 21.52 \pm 0.39 \qquad (S_a \to S_c)$$

$$\mu_0 = 22.61 \pm 0.39 \qquad (S_d)$$

TODO: How evolution can change the spiral:
Stelar Halo
MW, M31 $\Rightarrow \rho \propto r^{-3}$
If a galaxy is nearby and it is edge-on, we can see a thick disk.
the size of the disk is $\mu_B \sim 22.5 mag/arcsec^2$
Another important law is the **Law of Star Formation Rate** (Schmidt-Kennicutt Law):

$$\sum_{SFR} \propto \sum_{gas}^{N}$$

$$\frac{M_{\odot}}{ykpc^2}$$

Surface photometry bias

If we observe a portion of a galaxy, and we must ”look through” a portion of the galaxy we will see a redder light than observing it from an angle where we don’t have to ”look through” any portion of the galaxy.
The same happens for the bulge.
Let’s suppose a spiral with no dust: if we observe a ”face-on” galaxy, we will see a brighter galaxy than observing the same galaxy ”edge-on”.
If we consider a very dusty spiral instead, we will notice that the galaxy appears with a similar brightness in both face-on and edge-on views, due to the dust.

Rotation curves

The rotation curve is the curve that shows the velocity of the stars in the galaxy as a function of the distance from the center of the galaxy.
…
A part of this velocity is related to the baryonic mass.
We can decompose the velocity:
DM Halo disk
If $\frac{M}{L} \sim stars$ We do not need to consider Dark Matter in the disk. If $\frac{M}{L} \gg stars$ We need to consider Dark Matter in the disk.
In general, the max velocity is higher if the luminosity is higher. If we pick galaxies with the same luminosity, the max velocity is higher for the galaxies with the higher mass.
arms:
grand design -> density moves (internal) S_c flocculent -> tidal interaction (external)

3.1.1 Virial Theorem

[karttunen demonstration]
If a system is virialized, the following equation holds:

$$2T + U = 0$$

where T is the kinetic energy and U is the potential energy.
Suppose we have a system of n point masses m_i with radius vectors r_i and velocities $\dot{r}_i$. We define a quantity A (the “virial” of the system) as follows:

$$A = \sum_{i=1}^{n} m_i \dot{r}_i \cdot r_i$$

Time derivative:

$$\dot{A} = \sum_{i=1}^{n} (\underbrace{m_i \dot{r}_i \cdot \dot{r}_i}_{2T} + \underbrace{m_i \ddot{r}_i \cdot r_i}_{F_i})$$

$$\dot{A} = 2T + \sum_{i=1}^{n} nF_i \cdot r_i$$

Time average:

$$\langle \dot{A} \rangle = \frac{1}{\tau} \int_0^{\tau} \dot{A} dt = \langle 2T \rangle + \langle \sum_{i=1}^{n} F_i \cdot r_i \rangle$$

If the system remains bounded—that is, none of the particles escapes—all positions $\vec{r}_i$ and velocities $\dot{\vec{r}}_i$ stay finite. In this case, the virial A does not grow without bound, and the integral in the previous equation also remains finite. When we consider an increasingly long timespan ($\tau \to \infty$), the time average $\langle \dot{A} \rangle$ approaches zero, and we obtain:

$$\langle 2T \rangle + \langle \sum_{i=1}^{n} F_i \cdot r_i \rangle = 0$$

where F_i is the garvitational force:

$$\vec{F}_i = -Gm_i \sum_{j=1, j\neq i}^{n} m_j \frac{\vec{r}_i - \vec{r}_j}{r_{ij}^3}$$

where $r_{ij} = |\vec{r}_i - \vec{r}_j|$.
The latter term od the viral theorem becomes:

$$\begin{aligned} \textstyle\sum_{i=1}^{n} F_i \cdot r_i &= -G \textstyle\sum_{i=1}^{n} \sum_{j=1, j\neq i}^{n} m_i m_j \frac{r_i - r_j}{r_{ij}^3} \cdot r_i \\ &= -G \textstyle\sum_{i=1}^{n} \sum_{j=i+1}^{n} m_i m_j \frac{r_i - r_j}{r_{ij}^3} (r_i - r_j) \end{aligned}$$

Which is obtained combnining:

$$\begin{aligned} (1) &= -G \textstyle\sum_{i=1}^{n} \sum_{j=1, j\neq i}^{n} m_i m_j \frac{\vec{r}_i - \vec{r}_j}{r_{ij}^3} \cdot \vec{r}_i \\ (2) &= -G \textstyle\sum_{j=1}^{n} \sum_{i=1, i\neq j}^{n} m_i m_j \frac{\vec{r}_j - \vec{r}_i}{r_{ji}^3} \cdot \vec{r}_j \\ (3) &= -G \textstyle\sum\sum m_i m_j \frac{\vec{r}_i - \vec{r}_j}{r_{ij}^3} (-\vec{r}_j) \end{aligned}$$

…(maybee missing something)
we get:

$$\sum_{i=1}^{n} \vec{F}_i \vec{r}_i = -G \sum_{i=1}^{n} \sum_{j=i+1}^{n} \frac{m_i m_j}{r_{ij}} = U$$

From the virial theorem we want to derive ***observational quantities***.

$$\sum_i m_i (v_i - \langle v \rangle)^2 - G \sum_{i>j} \frac{m_i m_j}{r_{ij}} = 0$$

$$\underbrace{\frac{\sum_i m_i (v_i - \langle v \rangle)^2}{\sum_i m_i}}_{\text{velocity dispersion}} - G \underbrace{\frac{\sum_{i>j} \frac{m_i m_j}{r_{ij}}}{(\sum_i m_i)(\sum_i m_i)}}_{\equiv \frac{1}{R_v} \text{ viral radius}} \sum_i m_i = 0$$

...

2D position, 1D observations

$$\sigma_v^2 - G\frac{M}{R_v} = 0$$

$$M = \frac{\sigma_v^2 R_v}{G}$$

If the system is spherical, we can use the projected radius to get the virial radius.

$$\sigma_v^2 = 3\sigma_{v,los}^2$$

Therefore, we have:

$$R_v = \frac{\pi}{2} R_{v,projected}$$

$$M = \frac{3\pi}{2} \frac{\sigma_{v,los}^2 R_{v,projected}}{G}$$

Segregation effect: Some objects behaves differently: not always mass is proportional to luminosity. Therefore we need to use the formula above.
Sometimes we will see "tensorial virial theorem", and "generalized virial theorem".

Observation: ***Virial Theorem validity***

The viral theorem is valid if the mass follows the same distribution of light, buth this is not always the case.

The definition of the **viral radius** (or better, the *radius of the virial theorem*) is:

$$R_v = \frac{n^2}{\sum_{i>j} \frac{1}{r_{ij}}}$$

The **harmonic radius** is:

$$R_H = \frac{n(n-1)/2}{\sum_{i>j} \frac{1}{r_{ij}}}$$

Scaling relations - Spiral galaxies

The **Trully-Fisher relation** allows us to relate the luminosity of a galaxy to its velocity dispersion.

$$L \propto V_{max}^{\alpha} \qquad \alpha \sim 4$$

Calibrated TF relation fron nearby galaxies.
For distant galaxies, we can obtain the redshift from the spectrum, and the rotation velocity (and, in particular, V_{max}). Then we can calculate M, and then the distance from $m - M$.

- For nearby galaxies we can use cepheids to calculate de distance
- For very far galaxies we can use the Hubble law
- For the ones in the middle we can use the TF relation

VT + Spiral structure -> T-F relation

$$\mathscr{M} \propto \frac{V_{max}^2 R}{G} \left(\times \frac{L}{\mathscr{M}} \right)$$

so we get:

$$L \propto \left(\frac{\mathscr{M}}{L} \right)^{-1} \frac{V_{max}^2 R}{G}$$

$$L \propto \left(\frac{\mathscr{M}}{L} \right)^{-2} \frac{R^2}{LG^2} v_{max}^4$$

$$L^2 \propto \left(\frac{\mathscr{M}}{L} \right)^{-2} \frac{R^2}{G^2} v_{max}^4$$

$$L \propto \left(\frac{\mathscr{M}}{L} \right)^{-2} \left(\frac{1}{\langle I \rangle G^2} \right) v_{max}^4$$

$$\frac{\mathscr{M}}{L} \sim const$$

The Faber-Jackson relation

The fundamental plane

$$(R_e, \sigma_0, \langle I \rangle_e)$$

$$R_e \propto \sigma_0^{1.4} \langle I \rangle_e^{-0.85}$$

Virial Theorem + Kormendy Relation -> Fundamental Plane

$$R_e \propto \langle I \rangle_e^{-0.82} + \frac{\mathscr{M}}{L} \propto \mathscr{M}^{0.2}$$

The $D_n - \sigma$ Relation

Be D_n the diameter of an ellipse within the average surface brightness I_n corresponds to a value of $20.75 mag/arcsec^2$.
We have thet:

$$D_n \propto \sigma_0^{1.33}$$

Spectrum -> σ_0 -> D_n -> distance

Boh

1. Luminous galaxies $\rightarrow$ Hubble types
2. Elliptical $\neq$ Spiral galaxies
   - morphology
   - kinematics
   - gas content
   - SF (= color)
3. Kinematics
   - Spiral: ordered m^+, V_{max}
   - Ellipticals: random m, σ_v

3.2 Lecture 28/10/2025

Galaxies' luminosity function

The luminosity function $(\Phi(L))$ is the number of galaxies per unit volume per unit luminosity.

$$v = \int_{-\infty}^{\infty} \Phi(M)dM = \int_{0}^{\infty} \Phi(L)dL$$

We encounter different problems:

- what's the distance of a cluster of galaxies?
- large scale structure
- Maluquist bias - limited surveys in m

TODO: reproduce plot in the notebook

During the years, multiple attempts to solve the problem have been made:

- Press-Schechter (74) halos -> Mass function
- Schechter (79) -> Luminosity function

$$\Phi(L) = \left(\frac{\Phi^*}{L^*}\right)\left(\frac{L}{L^*}\right)^{\alpha} e^{-\left(\frac{L}{L^*}\right)}$$

where $\alpha \sim -1$
thypical B-band:

$$\Phi^* = 1.6 \cdot 10^{-2}\{h^{+3}\}$$

$$M_B^* = -19.7 + 5\log h \quad \Leftarrow \quad L_B^* = 1.2 \cdot 10^{10} h^{-2} L_{\odot,B}$$

Therefore, $\alpha = -1.07$
For K-band:

$$\Phi_K^* = 1.6 \cdot 10^{-2} Mpc^{-3}$$

$$M_K^* = -23.1$$

therefore, $\alpha = -0.9$

Observation: h^{+3}

h^{+3} is used to rescale the luminosity function. At first it was related to $\Omega_m \sim 1$, nowadays it is not so easy to determine, and it depends on H_0.

$$L_{tot} = \int_0^{\infty} dL\Phi(L)L = \Phi^* L^* \Gamma(2+\alpha)$$

which is finite for $\alpha \geq -2$

$$N_{tot} = \int_0^{\infty} \Phi(L)dL$$

which is finite for $\alpha > -1$

The 60% of L_{tot} is contained in the range $0.22L^* < L < 1.6L^*$
The 90% of L_{tot} is contained in the range $0.1L^* < L < 2.3L^*$
Typical luminosity of galaxies is $\Phi^* \sim 2 \cdot 10^{-2} Mpc^{-3}$, with an average separation of $4Mpc$.
In clusters, the density is way higher than in the field (the rest of the universe). In fact, the average distance between galaxies is $\sim 1 - 2Mpc$.

Specific Luminosity Function

LF for morphological types:

Field

TODO: put here plot (a) sheet G14 Fig 3.51

Clusters

TODO: put here plot (b) sheet G14 Fig 3.51

In general it is valid $L_{s\emptyset} > L_{sa}$ - Lenticular galaxies are brighter than spiral galaxies.
Effects due to evolution of galaxies:
A merge of spiral galaxies can result in an elliptical galaxy $S + S \to E$

Groups

- $N \lesssim 50$ galaxies
- $M \lesssim 3 \cdot 10^{13} M_\odot$
- $T_x \sim 1 \to 3KeV$
- $\sigma_v \sim 200 \to 300 km/s$

Clusters

- $N \gtrsim 50$ galaxies
- $M \gtrsim 3 \cdot 10^{14} M_\odot$
- $T_x \sim 4 \to 10KeV$
- $\sigma_v \sim 400 \to 1000 km/s$

$$R_{Abell} = 1.5 h_{100}^{-1} Mpc \quad \to \quad 1.5 \cdot \frac{100}{70} h_{70}^{-1} M_r$$

Both are composed mainly by:

- Stars $\sim 3 - 5\%$
- Hot gas $(3 \cdot 10^7 K) \sim 15 - 20\%$
- Dark Matter $\sim 80\%$

Galaxy distribution

The following figure shows the distribution of galaxies in the universe.

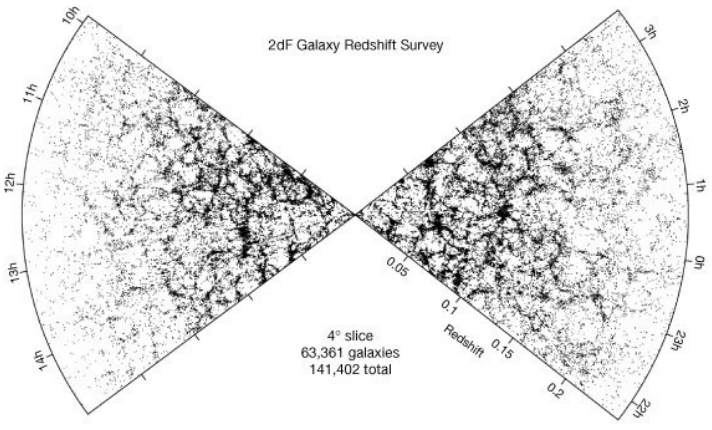

Some structures are "real", such as the *Great Wall*, others are "apparent", such as the *Finger of God*.

Tip: ***Galaxy distribution***

In high redshift zones, the galaxies seem to be less dense than in low redshift zones. This is because the farthest galaxies have a lower apparent magnitude than the nearest ones.

4
Lecture 30/10/2025

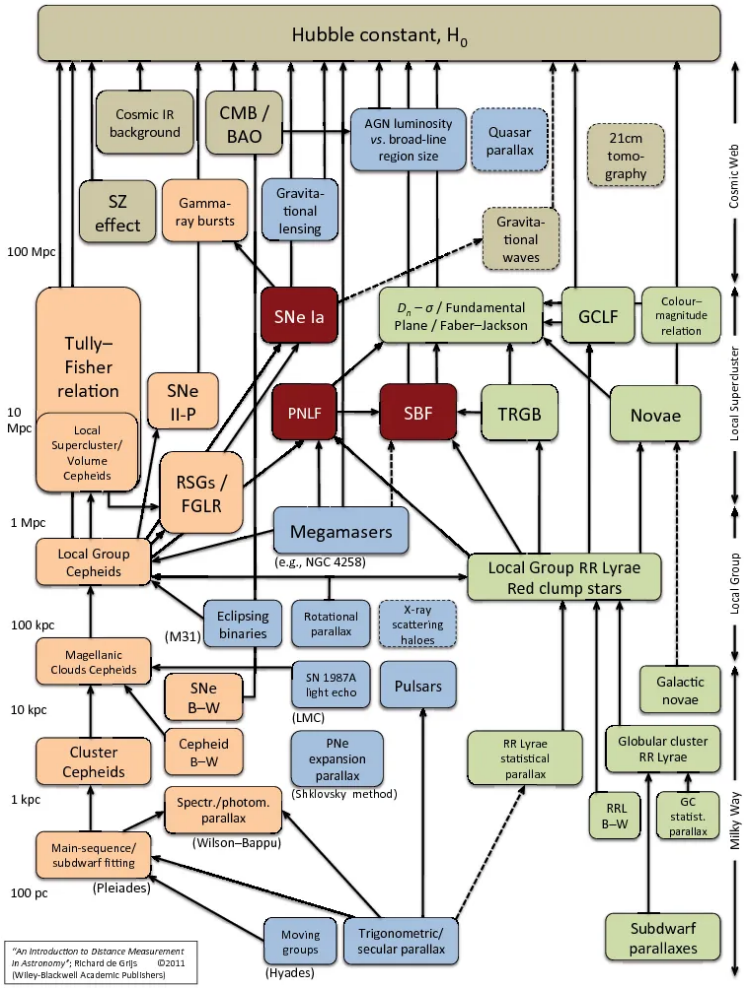

Figure 4.1: The distance ladder

MISSING: something

$$\Delta R = R_1 - R_0 = p \int_{T_0}^{T_1} v(t)dt$$

$$m_1 - m_0 = M_1 - M_0 = -5[\log(R_0 + \Delta R) - \log R_0] = -10[\log T_1 - \log T_0]$$

$$R_0 = f(m_0, m_1, \Delta R, T_0, T_1)$$

Surface Brightness Fluctuations (SBF):

$$z \sim 0 \qquad \rightarrow \qquad SB \sim const$$

Galaxy nearby have a small number N of stars, while galaxies far away have a large number N of stars.
The poissonian error goes $\sim \sqrt{N}$
The relative error is $\sim \frac{\sqrt{N}}{N}$
Supernovae: you can obtain $\Delta t \sim L_{max}$ from the light curve. L_{max} results in the absolute magnitude of the supernova, summing up the apparent magnitude of the supernova we can find the distance modulus.
Hubble law (1928):

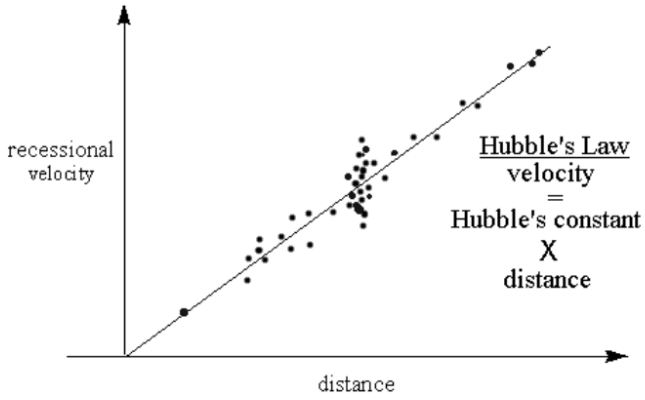

Figure 4.2: Hubble law (1929)

$$v = H_0 d$$

what is H_0?
In 1990:
- **optical** $H_0 = 50 \frac{km}{s}/Mpc$
- **x-ray** $H_0 = 100 \frac{km}{s}/Mpc$

CMB (MW background cosmology): $H_0 \sim 70 \frac{km}{s}/Mpc$

$$H_0 = h \cdot 100 \frac{km}{s}/Mpc$$

MISSING: something

Observation: ***Cluster in Hubble's Law***

In the Hubble's Law graph, the "vertical" spread of data points, depicted as clusters known as the "Finger of God", arises from galaxy clusters' peculiar velocities. These formations do not reflect any true spatial structure in the universe.

Distant Clusters

$$E(z) = \frac{H(z)}{H_0}$$

closure of the universe:

$$\rho_c = \frac{3H_0^2}{8\pi G}$$

Galaxies in principle are expanding, at some point they are in a region where the average density is higher than the critical density, and they start to collapse.

$$\langle \rho \rangle > \rho_c \qquad \Rightarrow \qquad \langle \rho \rangle = 20\rho_c$$

In order to define a size of a cluster, we have to define radius such as R_{200}.

$\gtrsim 50\%$ of the galaxies stays in groups, not in clusters.
$\sim 5\%$ of the galaxies stays in clusters.
In the local group there are about 35-50 galaxies. $L < L^*$

	MW	M31	M33
L^*	SB_{bc}	S_b	S_c
M_B	-20	-21.2	-18.9

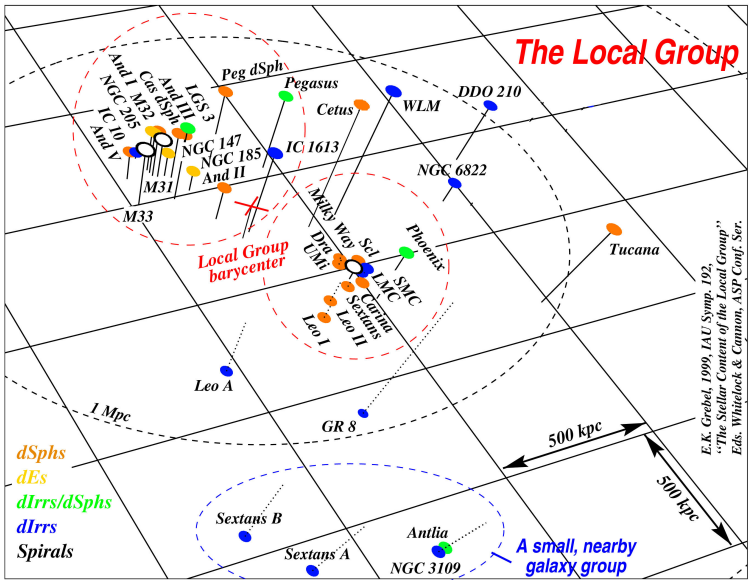

Figure 4.3: Local group [1]

$$V \sim -120 Km/s, \qquad D = 770 Kpc, \qquad \text{collisions in } 6 \cdot 10^9 years$$

The mass of the Local Group is:

$$M \sim 3 \cdot 10^12 M_\odot$$

We can use a two body model to calculate the mass of the Local Group.

$$M_{LG} = M_{MW} + M_{M31} \sim 90\% L_{LG} \sim 90\% M_{LG}$$

Let's consider at $t = 0$ the two galaxies are very close to each other and they are moving far away from each other.
they will reach a maximum distance r_max at time t_max where $v_max = 0$. Then they start to collapse again.

$$\frac{1}{2} M v^2 - \frac{GM^2}{r} = c$$

$$C = -\frac{GM^2}{r_max}$$

$$\frac{1}{2}\left(\frac{dr}{dt}\right)^2 = \frac{GM}{r} - \frac{GM}{r_max}$$

$$(dt)^2 = \frac{(dr)^2}{2GM}\left(\frac{1}{\frac{1}{r}-\frac{1}{r_max}}\right)$$

$$dt = \frac{dr}{\sqrt{2GM}}\frac{1}{\sqrt{\frac{1}{r}-\frac{1}{r_max}}}$$

$$t_max = \int_0^{t_{max}} dt = \int_0^{r_{max}} \frac{dr}{\sqrt{2GM}\sqrt{\frac{1}{r}-\frac{1}{r_max}}} = \frac{\pi}{2}\frac{r_{max}^{3/2}}{\sqrt{2GM}}$$

where the result is obtained using the Wolfram rule:

$$\int_0^a \frac{1}{\sqrt{\frac{1}{x}-\frac{1}{a}}}dx = \frac{\pi}{2}a^{3/2}$$

Thus, r_max is obtained by solving the equation:

$$r_{max} = \left(\frac{2\sqrt{2GM}}{\pi}t_{max}\right)^{2/3}$$

$$\frac{v^2}{2} = \frac{GM}{r} - \frac{1}{2}\left(\frac{\pi GM}{t_max}\right)^{2/3}$$

$$v = f(M, t_{max}) \quad \rightarrow \quad M = f(v, t_{max}) = 3\cdot 10^12 M_\odot$$

MISSING: something

$$t_{max} \sim \frac{T_0}{2} + \frac{D_{obs}}{2V_{obs}} \sim 10^10 years$$

Sculptor Group has a distance of 1.8 Mpc and it is composed by 6 galaxies
M81 group has a distance of 3.5 Mpc and it is composed by 8 galaxies
Virgo cluster has a distance of 16 Mpc and it is composed by 250 galaxies, it occupies 10° of space in the sky. Its most important galaxy is M87.
Coma Cluster has a distance of 90Mpc, a redshift of $z \sim 0.03$

4.0.1 Catalogues of clusters

optical: Sovradensity of galaxies
An important catalog of galaxy clusters is the *Zwicky catalogue* (1961-68), which contains more clusters, but for which the applied selection criteria are considered less reliable.
The *Abell catalogue* (1958-89) contains $N_{gal} \geq 50$ galaxies.
Those 50 galaxies have a magnitude in the following range:

$$m_3 \leq m \leq m_3 + 2$$

But also a radius such that:

$$\theta_A = \frac{1.7'}{z}$$

Therefore:

$$R_{Abel} = 1.5h^{-1}Mpc$$

The *Abell Corwin & Olowin catalogue* (ACO) contains around 4000 clusters (with a small redshift $z < 0.2$)

Problems with the catalogues

The selection of galaxy clusters from an overdensity of galaxies on the sphere is not without problems, in particular if these catalogs are to be used for statistical purposes.
We have two main problems:
We need to define two quantities:

- **Completeness**: $\frac{N_{obs}}{N_{true}} \leq 1$
- **Purity**: $\frac{N_{obs} - N_{false}}{N_{obs}} \leq 1$

A galaxy cluster is a three-dimensional object, whereas galaxy counts on images are necessarily based on the projection of galaxy positions onto the sky.
Therefore, projection effects are inevitable. Random overdensities on the sphere caused by line-of-sight projection may easily be classified as clusters. These so-called *projection effects* are the most serious problem with the catalogues.

4.0.2 Morphological Classification

The morphological classification of galaxy clusters by Rood and Sastry is defined by several categories:

- **cD**: Clusters categorized as cDs are characterized by the dominance of a central *cD galaxy*.
- **B**: Clusters categorized as Bs are distinguished by a ***binary*** system of bright galaxies at their center.
- **L**: Clusters categorized as Ls exhibit a nearly ***linear*** alignment of their dominant galaxies.
- **C**: Clusters categorized as Cs are identified by a ***single core*** of galaxies.
- **F**: Clusters categorized as Fs are described as having a ***flat*** galaxy distribution.
- **I**: Clusters categorized as Is are notable for their ***irregular*** distribution.

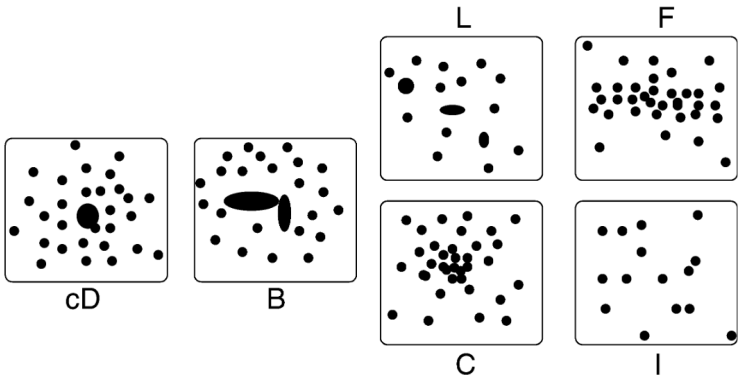

Figure 4.4: Morphological classification by Rood and Sastry [3]

MISSING: a lot of stuff
Modern Catalogues
Bautz-Morgan:
sovraddensity of galaxies
Color magnitude diagram
…

- sovraddensity of galaxies
- color magnitude diagram

…
Max BCG catalog (SDSS survey):
This catalog is 90% pure and 85% complete. $M \geq 10^{14} M_{\odot}$

- red sequence
- dominant central galaxy
- radial profile of galaxies distribution

4.0.3 Groups

- **Loose Groups**
  They are the most common type of groups, they include almost the 50% of the galaxies.
- **Compact Groups**
  They are very rare.
  This is the case where we have a high density of galaxies, and they are all close to each other.

$$t_{dyn} \sim \frac{R}{\sigma_v} \sim 0.02 H_0^{-1}$$

- **Fossil Groups**

$$\Delta m_{12} \geq 2 mag$$

Tip: ***Fossil Groups***

The name fossil depends of the fact that a researcher thought it was the first group ever formed in the universe.

5 Lecture 04/11/2025

MISSING: Start of the lecture

The Inter Cluster Medium (ICM) is the hot gas that fills the space between the clusters. Between 1920 and 1933 were discovered the first X-ray sources.

Telescopes:

- X-ray (mono source, then extended source)
- UMURU
- Einstein
- Rosat
- Chandra
- XMM
- E-Rosat
- Athena

Athena to study the motion of the gas in some clusters

$$L_X \sim 10^{43-45} erg/s$$

FF emission: Bremsstrahlung

- Groups $kT \sim 1-3KeV$
- Clusters $kT \sim 10-12KeV$ (at least $> 4-5KeV$)

$$E_\nu \equiv \frac{dL}{dV d\nu}$$

$$e_\nu^{ff} \propto \underbrace{n_e n_i}_{n_e^2} T^{-1/2} e^{-\frac{h\nu}{kT}}$$

TODO: insert plots from paper sheets A2 (right column)

$$E \propto \sqrt{T} n_e^2 \qquad KT \gtrsim 5KeV$$

ff+bf+bb:

$$E \propto T^{-0.6} n_e^2 \qquad KT \leq 2KeV$$

Rosat has a sensibility range of $0.1-2.4KeV$. It is very useful to measure the mass of a cluster.

If the gas is homogeneous, we have: $\langle n_e^2 \rangle = \langle n_e \rangle^2$, but if the mass is not homogeneous, we have: $\langle n_e^2 \rangle \neq \langle n_e \rangle^2$.

From observations we can note that the gas mass is much smaller than the stellar mass: $M_g as \sim 5-10 M_\star$. An important indicator is the following ratio:

$$\frac{M_{gas}\ (\sim 15-20\% M_{tot})}{M_\star\ (\sim 3-5\% M_{tot})}$$

The higher is the total mass M_{tot}, the higher is the ratio $\frac{M_{gas}}{M_\star}$.
A conclusion is that clusters are richer in gas, while groups are richer in stars. Follows that the clusters retain better the gas, and the groups are more efficient in forming stars.
Since $e_x \propto n_e^2$, the x-ray emission comes from the core of the cluster, therefore you can have a better view of where the cluster is in space (for distances $< 1Mpc$). There is still the problem of the flux limit.

Clusters morphology

We can find different morphologies for the clusters:
- **Unimodal Clusters**: they have a single peak in the x-ray emission.
- **Bimodal Clusters**: they have two peaks in the x-ray emission.

We can talk further about substructures in the clusters.
Unimodal clusters
$\beta - model$
- 3 dimensional profile:

$$\rho_{gas}(r) = \rho_{0,gas}\left(1+\left(\frac{r}{\beta r_{c,gas}}\right)^2\right)^{-\frac{3}{2}\beta_{fit,gas}} \qquad \Rightarrow \qquad r^{-2}\beta_{fit,gas} = \frac{2}{3}$$

- 2 dimensional profile:

$$\Sigma_{gas}(R) = \Sigma_{0,gas}\left(1+\left(\frac{r}{\beta R_{c,gas}}\right)^2\right)^{-\frac{3}{2}\beta_{fit,gas}+\frac{1}{2}} \qquad \Rightarrow \qquad R^{-1}$$

- observed profile:

$$S_x = S_{x,0}\left(1+\left(\frac{r}{\beta R_{c,gas}}\right)^2\right)^{-3\beta_{fit,gas}+\frac{1}{2}} \qquad \Rightarrow \qquad S_x = \int \rho_{gas}^2$$

We have a typical ICM density of:

$$n_e \sim \frac{1\cdot 10^{-3}}{cm^{-3}}$$

Cooling Flows (or, in older literature, Cool Cores) are clusters with a high density of gas in the center, characterized by a big emission in the center.

$$t_{cool} = \frac{\mu}{e_{ff}} \sim \underline{8.5\cdot 10^{10} yr}\left(\frac{n_e}{10^{-3}cm^{-3}}\right)\left(\frac{T_{gas}}{10^8 K}\right)$$

Which is bigger than the Hubble time $t_H \sim 13\cdot 10^9 yr$, therefore we have no cooling.

$$\omega = \frac{3}{2} n_e k T$$

$$E^{ff} \propto n_e^2 T^{1/2}$$

The center of some clusters can have high n_e and a lower $t_{cool} < t_H$, therefore we have a cooling core. In these kind of clusters we can observe star formation from the gas.
These kind of clusters have no big Surface Brightness …
MISSING: something about No Cool Core and Mergers

Sunyaev-Zel'dovich Effect

The Sunyaev-Zel'dovich Effect is a small distortion of the Cosmic Microwave Background Radiation (CMBR) due to the interaction with the ICM.

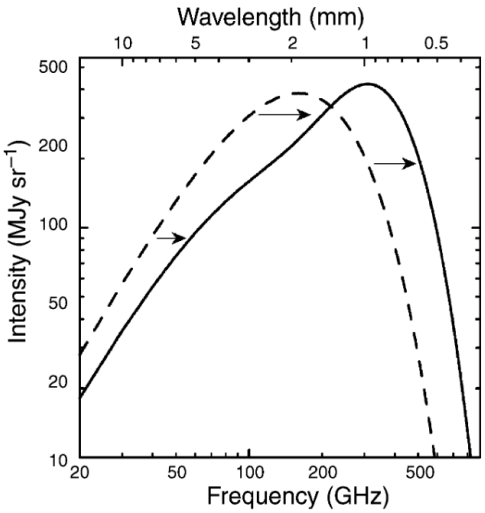

Figure 5.1: Sunyaev-Zel'dovich Effect [3]

In the Rayleigh-Jeans domain of the CMB spectrum, thus at wavelengths larger than about 1 mm, photons are effectively removed by the SZ effect. For the change in specific intensity in the RJ part, one obtains:

$$\frac{\Delta I_\nu^{RJ}}{I_\nu^{RJ}} = -2y$$

where y is the ***Compton-y parameter***:

$$y = \int_0^\infty dl \frac{kT_{gas}}{m_e c^2} \sigma_T n_e$$

and σ_T the Thomson cross-section for electron scattering:

$$\sigma_T = \frac{8\pi}{3} \left(\frac{e^2}{m_e c^2} \right)^2$$

therefore:

- $y \propto$ optical depth
- $y \propto n_e$
- $y \propto T_{gas}$

So y can be a proxy for cluster mass.

$$\theta = \frac{R}{D_A}, \quad d\theta = \frac{dR}{D_A}$$

$$sz - eff = \int d^2\theta y = \frac{1}{D_A^2} \int d^2 R y \propto \frac{1}{D_A^2} \int dV n_e T_{gas}$$

$$Y_{sz} \equiv M_{gas} \cdot T_{gas}$$

Radio extended emission

There are galaxies with very large radio halos ($\sim 1Mpc$ in size).
Radio Relics -> elongated halos, polarized light
synchrotron emission:
We have a (very weak) magnetic field B ($\leq 1\ \mu G$) and a gamma factor $\gamma \sim 10^4$
For instance, if $\gamma = 300$, then the electron energy is $E = \gamma m_e c^2 \sim 150MeV$.
But if we consider a time $T_{life} = 10^9$ its energy will be fewer and fewer.
protons instead have a shorter lifetime.
Bimodal clusters mergers can result in:

- **Shocks**:
  - $v_{rel} \sim 1 - 2 \cdot 10^3 km/s$
  - gravitational energy: 10^64erg
  - dissipation: $3 \cdot 10^63erg$
- **Turbulence**:
  - ...

MISSING: last few minutes of the lecture

6
Lecture 06/11/2025

Frequencies

VLA instruments works at a frequency of 1.4 GHz. while LOFAR has a range of 300-800 MHz.
They allow us to study phenomena such as mergers, with ratios 1:1 to 1:10.
They allow us also to study AGN and their radio emission. There are three main models:

- primary electrons models: not good because it (something with the scale)
- primary electron reacceleration models: good because it explains the radio emission of some clusters.
- secondary electron reacceleration models: no evidence of it.

Galaxies and X-ray emission

Sarazin 1986-88 did a lot of studies and pubblications about the X-ray emission of galaxies.
ICM
We assume that the gas in the cluster is adiabatic (= isotropic)
We remember that for an ideal gas it holds that:

$$pV = n_{mol}RT = n_{mol}\mathcal{N}\frac{R}{\mathcal{R}}T$$

so we get:

$$pV = NK_BT \qquad \Rightarrow \qquad p = \frac{NK_BT}{V}$$

$$\rho_{gas} = \rho = n\langle m\rangle = n\mu m_p$$

we can define μ as the mean atomic mass:

$$\mu \equiv \frac{\langle m\rangle}{m_p} \sim 0.6$$

therefore, we get:

$$\boxed{p = \rho\frac{K_BT}{\mu m_p}}$$

in an isothermal situation, we have:

$$p = k\rho$$

And in an adiabatic situation, we have:

$$p = k^i\rho^\gamma$$

where $\gamma = \frac{c_p}{c_v} = \frac{5}{3}$ for a monatomic gas.

Hydrostatic equilibrium

We can observe that the cluster is in hydrostatic equilibrium:

$$t_{sc} = \frac{2R_A}{c_s}, \qquad c_s^2 = \left.\frac{dp}{d\rho}\right|_{\rho=\rho_0}$$

where c_s is the sound speed:

$$c_s \sim \sqrt{\frac{p}{\rho}} = \sqrt{\frac{nK_BT}{\mu m_p}} \sim \sqrt{1000 km/s}$$

Therefore we observe a value of t_sc smaller than the Hubble time (time of the universe):

$$t_{sc} \sim 7 \cdot 10^8 yr < 13 \cdot 10^9 yr = t_H$$

—

$$\vec{\nabla} p = -\rho \vec{\nabla} \phi$$

sphere:

$$\frac{dp}{dr} = -\rho \frac{GM(r)}{r^2}$$

to convince us:

$$p = \frac{F}{A} \quad \Rightarrow \quad \frac{p}{x} = \frac{F}{V}$$

so

$$\vec{\nabla} p \cdot V = -m \vec{\nabla} \phi \qquad \Rightarrow \qquad \vec{\nabla} p = -\rho \vec{\nabla} \phi$$

Coming back, we have:

$$\frac{GM(r)}{r^2} = -\frac{1}{\rho} \frac{K}{\mu m_p} \left(\rho \frac{dT}{dr} + T \frac{d\rho}{dr} \right)$$

$$M(r) = -\frac{1}{G} \left(\frac{KT}{\mu m_p} \right) r \left[\frac{d \ln \rho_{gas}}{d \ln r} + \frac{d \ln T}{d \ln r} \right]$$

In a 3D situation, we have:

$$\rho_{gas}(r) = \rho_{gas,0} \left(1 + \left(\frac{r}{r_{c,gas}} \right)^2 \right)^{-\frac{3}{2} \underbrace{\beta_{fit,gas}}_{\sim 2/3}}$$

where, if $r \gg r_{c,gas}$, we have $\rho \to r^{-2}$.

For galaxies, we have - Jeans Equation:

$$M(r) = -\frac{1}{G} \sigma_r^2 r \left[\frac{d \ln \rho_{gas}}{d \ln r} + \frac{d \ln \sigma_r^2}{d \ln r} + 2\beta \right]$$

Where the factor β is called *the velocity anisotropy parameter*.

$$\beta(r) = 1 - \frac{\sigma_\tau^2}{\sigma_r^2}, \qquad \text{where} \quad \sigma_\tau^2 = \frac{\sigma_\theta^2 + \sigma_\phi^2}{2}$$

for an isotropic orbit, gas is a collisional component, therefore we have:

$$\boxed{\beta(r) = 0}$$

so the *number density* of a galaxy is:

$$\rho_{gal}(r) = \rho_{gal,0}\left(1 + \left(\frac{r}{r_{c,gal}}\right)^2\right)^{-\frac{3}{2}\beta_{fit,gal}}$$

historically, $\beta_{fit,gal} = 1$ was used.
We can derive the Jeans Equation for galaxies:

$$\frac{-KT}{\mu m_p}\frac{d\ln\rho_{gal}}{dr} = -\sigma_r^2\frac{d\ln\rho_{gal}}{dr} - \frac{2\beta\sigma_r^2}{r}$$

$$\frac{\dfrac{d\ln\rho_{gal}}{dr}}{\dfrac{d\ln\rho_{gal}}{dr} + \dfrac{2\beta}{r}} = -\frac{\sigma_r^2}{\dfrac{KT}{\mu m_p}}$$

so we get:

$$\beta_{spec} = \frac{\sigma_{LOS}^2}{\dfrac{KT}{\mu m_p}}$$

$$\frac{d\ln\rho_{gal}}{dr} = \frac{1}{\rho}\frac{d\rho}{dr} = \ldots = -3\beta_{fit}\left(1 + \left(\frac{r}{r_0}\right)^2\right)^{-1} r$$

where, for $r \gg r_0$, we have $-3\beta_{fit}r^{-1}$.
MISSING: few calculations of the end of the first beta problem

Second beta problem

The second β problem still does not have commonly accepted solutions.

$$\beta_{spec} = \frac{\sigma_{LOS}^2}{\dfrac{KT}{\mu m_p}} \sim 1$$

The energy per unit mass for galaxies and for gas is the same.
equilibrium of energy for unit mass:

$$\frac{1}{2}mv^2 = \frac{3}{2}KT$$

in 1D:

$$\frac{1}{2}3\sigma_{1D}^2 = \frac{3}{2}KT$$

Violent relaxation - Lynden-Bell (1967)
They proposed that galaxies and gas forms together clusters, and they are in violent relaxation.
We can observe that the beta fitted is not the same as the beta spec.
solutions:

- **dynamical friction**: more important in groups
- **Inter-groups medium**: the energy of AGN is smaller than the energy of the ICM, but $T_{AGN} \sim T_{IGM}$
- **member selection in groups**

Galaxies in clusters

Morphology density relation - Dressler (1980)
Color-density relation
BCG: Brightest Cluster Galaxy
cD galaxies: E + light envelope (ICL = Inter-Cluster Light)
…
$v_{BCG} \sim \bar{v}$
coevolution of clusters and BCG (which is inside)

—

hypothesis of BCG formation:

- **merger**: cannibalism dynamics
- **no-limit tidal radius**: ...
- **cool core**: ...

...
we have two types of segregation:

- **Luminosity segregation in position**: more evident in clusters with a high density of galaxies
- **Luminosity segregation in velocity**: even a smaller effect ...

MISSING: Lecture before 13/11/2025

7 Lecture 13/11/2025

MISSING: start of the lecture
The Butcher-Oemler Effect is a scientific hypothesis suggesting the cores of galaxy clusters at intermediate redshift (z ~0.3) contain a larger fraction of blue galaxies than do the cores of low redshift clusters.
For high redshift it is observed that the fraction of cool cores is lower than in low redshift clusters.
Ths is valid if we have no observational bias.

7.1 Protoclusters

Protoclusters are ***condensation of galaxies*** that are not yet clusters. There is a gravitational force that is able to hold the galaxies together, but there is no equilibrium.
color-magnitude methods are not optimal to study protoclusters.
Also L_x id not optimal to study protoclusters.
Radiogalaxies and AGNs reveal the presence of a Protocluster.

Cluster mass

- VT (gals)
- hydrostatic equilibrium (ICM)
- SZ effect
- Gravitational lensing (GL)

Gravitational Lensing (GL) is a technique that allows us to study the mass distribution of a cluster by observing the distortion of the images of distant galaxies.
In a situation of strong lensing, when we observe to an image using the GL, we can see a little arc around the galaxy. This arc is due to the bending of the light by the mass of the cluster.
What we really see is the projection of the mass within the radius R of the cluster, along the line of sight.

$$\Sigma = \frac{c^2}{4\pi G}\frac{D}{D_L D_s}$$

where D is the distance between the observer and the cluster, D_L is the distance between the observer and the lens, and D_s is the distance between the lens and the source.
This effect is independent from the dynamic of the cluster
TODO: insert image 2.21 schneider book page 65
If we are in a situation of weak lensing, we can see another effect: …

Inter-Clusters Light (ICL)

It is supposed that the ICL follows the same distribution of the mass of the cluster.

In a cluster, glasxies are collisionless components, the gas is collisional and the dark matter, which follows the galaxies, is collisionless.
The bullet cluster is a good example of this. In this cluster, we can see the separation between the gas and the galaxies. The gas is like a shock wave that has passed through the cluster.
TODO: include plot in slides slidesClustersObsMassML - 19

8 Lecture 20/11/2025

$$W = -4\pi G \int dr \rho(r) M(r)$$

Poisson equation:

$$D^2\phi = 4\pi G\rho$$

$$\nabla^2\phi = \frac{1}{r^2}\frac{d}{dr}\left(r^2\frac{d\phi}{dr}\right) = 4\pi G\rho$$

Let's see some example of this spherical systems:

Example: ***Point mass***

$$\phi(r) = -\frac{GM}{r}$$

The circular velocity is:

$$v_c = \sqrt{\frac{GM}{r}}$$

The escape velocity is:

$$v_e = \sqrt{\frac{2GM}{r}}$$

We will have a decreasing circular velocity.

Example: ***Homogeneous sphere***

$$\rho(r) = \rho_0 \quad \text{for } r < R$$
$$\rho(r) = 0 \quad \text{for } r > R$$

The circular velocity is:

$$v_c^2 = \frac{GM}{r} = \frac{G\frac{4}{3}\pi R^3\rho_0}{r} = \frac{4\pi G\rho_0}{3}r^2$$

The caracteristic time:

$$T = \frac{2\pi r}{v_c} = \sqrt{\frac{3\pi}{G\rho}} = \sqrt{3\pi}\underbrace{(G\rho)^{-1/2}}_{\text{dynamical time}}$$

$$\Phi = \begin{cases} -2\pi G\rho(a^2 - \frac{1}{3}r^2) & \text{for } r < a \\ -\dfrac{4\pi G\rho a^3}{3r} & \text{for } r > a \end{cases}$$

Example: ***Plummer model***

This model is a good approximation for the mass distribution of the globular clusters.

$$\rho \sim const \quad \text{center of the cluster}$$

$$\rho \to 0 \quad \text{for } r \to \infty$$

$$\begin{cases} \Phi \propto r^2 + const & \text{for } r < a \\ \Phi \propto r^{-1} & \text{for } r > a \end{cases}$$

$$\Phi = -\frac{GM}{\sqrt{r^2 + b^2}}$$

2.44
Plummer scale

Example: ***Poisson equation***

$$\Phi \to \rho$$

$$\nabla^2\Phi = \frac{3GMb^2}{(r^2 + b^2)^{5/2}} = 4\pi\rho$$

$$\rho \to r^{-5}, \quad \text{for } r \gg b$$

Example: ***modification of Hubble model***

todo

Example: ***Power Law Density***

$$\rho(r) = \rho_0 \left(\frac{r_0}{r}\right)^{\alpha}$$

$$M = \int_0^{\infty} dr' 4\pi r'^2 \rho(r') = 4\pi\rho_0^{\alpha} \left. \frac{r'^{3-\alpha}}{3-\alpha} \right|_0^{\infty}$$

Example: ***Singular isothermal***

$\alpha = 2$ is a good approximation for the ICM.

$$\rho(r) = \rho_o \left(\frac{r_o}{r}\right)^2$$

$$\rho \to r^{-2}, \quad \text{for } r \to 0$$

$$\rho_{gas}^{ICM}$$

$$v_c^2 = \frac{GM(r)}{r} = \frac{4\pi G 1 rho_o r_0^{\alpha}}{3-\alpha} r^{2-\alpha}$$

$$v_c \propto r^{\frac{2-\alpha}{2}}$$

Therefore, for $\alpha = 2$, v_c is constant.

Example: ***Two-power law density***

Instead of consider only a power law density model, we can consider two:

$$\rho(r) = \frac{\rho_o}{\left(\frac{r}{a}\right)^{\alpha}\left(1+\frac{r}{a}\right)^{\beta-\alpha}}$$

- **Jaffe**
  used this model to describe the Milky Way bulge in 1983.

$$\begin{cases} \alpha = 2 \\ \beta = 4 \end{cases} \Rightarrow \beta - \alpha = 2$$

$$\frac{\rho}{\left(\frac{r}{a}\right)^2\left(1+\frac{r}{a}\right)^2} \quad \Rightarrow \quad \begin{cases} r^{-4} & \text{for } r \to \infty \\ r^{-2}(r+a)^{-2} & \text{for } r \to 0 \end{cases}$$

- **Hernquist**
  used this model to describe the Milky Way halo in 1990.

$$\begin{cases} \alpha = 1 \\ \beta = 4 \end{cases} \Rightarrow \beta - \alpha = 3$$

$$\frac{\rho_0}{\left(\frac{r}{a}\right)\left(1+\frac{r}{a}\right)^3} \quad \Rightarrow \quad \begin{cases} r^{-4} & \text{for } r \to \infty \\ r^{-3}(r+a)^{-3} & \text{for } r \to 0 \end{cases}$$

- **NFW**
  model (Navarro, Frenk, White in 1995) to describe the Dark Matter halo.

$$\begin{cases} \alpha = 1 \\ \beta = 3 \end{cases} \Rightarrow \beta - \alpha = 2$$

$$\frac{\rho_0}{\left(\frac{r}{a}\right)\left(1+\frac{r}{a}\right)^2} \quad \Rightarrow \quad \begin{cases} r^{-3} & \text{for } r \to \infty \\ r^{-1}(r+a)^{-2} & \text{for } r \to 0 \end{cases}$$

Einasto model

$$\rho(r) = \rho_0 \exp\left(-\left(\frac{r}{a}\right)^{\frac{1}{m}}\right)$$

therefore:

$$\begin{cases} \rho \to finite & \text{for } r \to 0 \\ M \to finite & \text{for } r \to \infty \end{cases}$$

Tip: ***In practice***

NFW model is easier and more used.

Fluid Mechanics

We have:
- a density $\rho(\bar{x},t)$,
- a pressure $p(\bar{x},t)$,
- a velocity field $\bar{v}(\bar{x},t)$.
- a thermodynamic funciton $T(\bar{x},t)$ or a specific entropy (entropy per unit mass) $s(\bar{x},t)$.

continuity equations:

$$M(t) = \int_V \rho(\bar{x},t) d^3x$$

let's suppose now that the mass changes with time:

$$\frac{dM(t)}{dt} = \int_V \frac{\partial \rho(\bar{x},t)}{\partial t} d^3x = -\int_S \rho \bar{v} d^2\bar{s}$$

Now we can write the continuity equation as:

$$\int_V \frac{\partial \rho}{\partial t} d^3x + \int_S \rho \bar{v} d^2\bar{s} = 0 \qquad \Rightarrow \qquad \int_V \frac{\partial \rho}{\partial t} + \bar{\nabla} \cdot (\rho \bar{v}) d^3\bar{x} = 0$$

$$\boxed{\frac{\partial \rho}{\partial t} + \bar{\nabla} \cdot (\rho \bar{v}) = 0}$$

Perturbation theory

Suppose that there is a small change in density due to a small movement of the fluid.
Let's consider an initial density ρ_0 and a small change at time $t_0 = 0$:

$$\rho_0 \to \rho(\bar{x}) \equiv \rho_0 + \varepsilon \rho(\bar{x}), \quad \text{where } \varepsilon \ll 1$$

$$\bar{x}_0 \to \bar{x}_1 \equiv \bar{x}_0 + \varepsilon \xi(\bar{x})$$

$$\int_{t_0-\delta}^{t_0+\delta} \left(\frac{\partial \rho}{\partial t} + \bar{\nabla} \cdot (\rho \bar{v})\right) dt = 0$$

Therefore:

$$\rho_1 - \rho_0 + \bar{\nabla}\left(\int \rho \bar{v}\right) = 0 \qquad \Rightarrow \qquad \rho_1 - \rho_0 + \bar{\nabla}\left(\int \rho \frac{d\bar{x}}{dt}\right) = 0$$

Euler equation:
in an inviscid fluid, we gravitational force $\vec{F}_g$, but also the pressure gradient force $\vec{F}_p$ and they are in equilibrium.
Starting from the fundamental equation:

$$M\vec{a} = \vec{F}$$

The total force is:

$$M\frac{d\vec{v}}{dt} = -\underbrace{\int_S p d^2\bar{s}}_{\text{pressure force}} - \underbrace{M\vec{\nabla}\Phi}_{\text{gravity force}}$$

The divergence is:

$$\int_s p d^2\bar{s} = \int_V \nabla p d^3\bar{x}$$

$$\int_V \rho \frac{d\bar{v}}{dt} d^3\bar{x} = -\int_V \bar{\nabla} p d^3\bar{x} - \int_V \rho \bar{\nabla}\Phi d^3\bar{x}$$

$$\rho\frac{d\bar{v}}{dt} = -\bar{\nabla}p - \rho\bar{\nabla}\Phi$$

$$\frac{d\bar{v}}{dt} = \frac{\partial\bar{v}}{\partial t} + \sum_{i=1}^{3}\frac{\partial\bar{v}_i}{\partial x_i}\frac{dx_i}{dt} = \frac{\partial\bar{v}}{\partial t} + (\bar{v}\bar{\nabla})\bar{v}(\nabla\bar{v})$$

$$\frac{\partial\bar{v}}{\partial t} + (\bar{v}\bar{\nabla})\bar{v} = -\frac{1}{\rho}\bar{\nabla}p - \bar{\nabla}\Phi$$

where compares the rate moomentum exit, and the rate momentum added to the volume.
In situations where a fluid is in hydrostatic equilibrium, the force due to the gradient of pressure balances exactly the gravitational force. This balance is mathematically expressed by the following equation:

$$\bar{\nabla}\Phi = -\frac{1}{\rho}\bar{\nabla}p$$

$$P = p(\rho, T) \qquad p = p(\rho, s)$$

Barotropic fluid:

$$p = p(\rho)$$

specific entropy is defined as:

$$dh = \frac{dp}{\rho}, \qquad h(\rho) = \int \frac{dp}{\rho'} = \int_0^\rho \frac{dp(\rho')}{\rho'}\frac{d\rho'}{d\rho} = \int_0^\rho \frac{dp(\rho')}{\rho'}\frac{d\rho'}{rho'}$$

$$\frac{\partial \bar{v}}{\partial t} + (\bar{v}\bar{\nabla})\bar{v} = -\bar{\nabla}(h+\Phi)$$

which is the Euler equation for a barotropic fluid.

---

constant density

$$\rho = const \quad \Rightarrow \quad p = const$$

$$\bar{\nabla}\Phi = 0$$

small perturbations:

$$\rho(\bar{x},t) = \rho_0 + \varepsilon\rho_1(\bar{x},t)$$

…

$$\frac{\partial \rho_1}{\partial t^2} - \left(\frac{\partial p}{\partial \rho}\right)_{\rho_0} \nabla^2\rho_1 = 0$$

$$v_s \equiv \sqrt{\left.\frac{\partial p}{\partial \rho}\right|_{\rho_0}}$$

$$\frac{\partial^2 \rho_1}{\partial t^2} - v_s^2\nabla^2\rho_1 = 0$$

waves equation:

$$\rho_1 = A\cos(kx - \omega t)$$

where:
A is the amplitude, k is the wave number, ω is the angular frequency.

$$\frac{\partial^2 \rho_1}{\partial t^2} = ... = -A\omega^2\cos(kx-\omega t) \qquad \text{and} \qquad \frac{\partial^2 \rho_1}{\partial x^2} = ... = -k^2 A\cos(kx-\omega t)$$

- For an ***ideal gas***:

$$pv = nRT \qquad \Rightarrow \qquad p = \rho\frac{K_b T}{m} = \rho\frac{K_b T}{\mu m_p}$$

$$p = \rho\bar{v}_x^2 = \rho\bar{v}_y^2 = \rho\bar{v}_z^2$$

$$\bar{v}_x^2 = \bar{v}_y^2 = \bar{v}_z^2 = \frac{1}{3}v^2 = \frac{K_B T}{\mu m_p}$$

- for ***adiabatic isoentropic*** gas it is valid the polytropic equation of state:

$$p = k'\rho^\gamma, \qquad \text{where } \gamma = \frac{c_p}{c_v}$$

Relaxation time

$$\lambda = \frac{1}{n\sigma}$$

where n is the number density and $\sigma = \pi(2R_\odot)^2$ is the cross section, and $R_\odot = 7 \cdot 10^5 km = 2.3 \cdot 10^{-8} pc$ is the radius of the Sun.

$$\lambda = 2 \cdot 10^{14} pc$$

interval $\frac{\lambda}{v} \sim 10^{18} yr$ is the time between two collisions, which is much bigger than the time of the universe $(13 \cdot 10^9 yr)$

The relaxation time is the tima at we have a big change in the velocity $(\frac{\Delta v}{v} \sim 1)$

The gas is different from a stellar system
in gas $v \sim const$ and we have rapid changes due to collisions. In a stellar system we have gravity forces.

$$F \propto r^{-2} \qquad m \propto r^2$$

Field perturbing stars
TODO: copy graph in pen from red notebook

$$\begin{aligned} |\int d\bar{v}_\perp| \sim & \int_{-\infty}^{+\infty} \frac{Gm}{b^2} (\cdots)^{-3/2} dt \\ \sim & \frac{Gm}{b^2} \frac{b}{v} \int_{-\infty}^{+\infty} (1+s^2)^{-3/2} ds \\ \sim & \frac{Gm}{b^2} \frac{b}{v} \left| \frac{s}{\sqrt{s^2+1}} \right|_{-\infty}^{+\infty} = \frac{Gm}{b^2} \frac{b}{v} \cdot 2 \end{aligned}$$

$$\left| \int d\bar{v}_\perp \right| \sim \delta v_\perp \sim 2 \underbrace{\frac{Gm}{b^2}}_{\text{max acc}} \overbrace{\frac{b}{v}}^{\text{encounter time}}$$

…

$$\delta n = \frac{N}{\pi R^2} 2\pi b db = \frac{2N}{R^2} b db$$

$$\delta v_\perp^2 \sim \int_{b_{min}}^{R} \delta v_\perp^2 \sim gN \frac{G^2 m^2}{v^2 R^2} \int_{b_{min}}^{R} \frac{\not{b}}{b^{\not{2}}} db = gN \frac{Gm}{Rv} \ln\left(\frac{R}{b_{min}}\right) \sim gN \frac{Gm}{Rv} \underbrace{\ln \lambda}_{\text{coulomb log}}$$

We can use the viral theorem:

$$Nm \sim \frac{v^2 R}{G}$$

$$v^2 \sim \frac{GNm}{R}$$

Therefore:

$$R \sim \frac{GNm}{v^2}$$

…

$$\frac{\Delta v_\perp^2}{v^2} \sim \frac{8NG^2m^2}{G^2N^2m^2} \ln \lambda$$

...

	n	n_{rel}	R	V **(km/s)**	**rel. time**	**notes**
Galaxies	10^{11}	$\sim 5 \cdot 10^8$	10 kpc	10^2	$5 \cdot 10^{16}$ yr	no collision
Globular clusters	10^5	$\sim 10^3$	10 pc	10	10^9 yr	collision
Galaxy clusters	10^3	15	1 Mpc	10^3	$1.5 \cdot 10^{10}$ yr	core: no collision outskirts: collision
Galaxy groups	10	0.5	≤ 0.5 Mpc	10^2	$2 \cdot 10^9$ yr	collision

9
27/11/2025

The Jeans Equations

…

$$M = -\frac{2\sigma_r^2}{G}\left(\frac{d\ln\nu}{d\ln r} + \frac{d\ln\sigma_r^2}{d\ln r} + 2\beta\right)$$

…

MISSING: start of the lecture

…

Observations:

$$\Sigma(R) = 2\int_0^\infty \nu(r)dz = 2\int_R^\infty \frac{\nu r}{\sqrt{r^2-R^2}}dz$$

…

What we measure from observations is a combination of the projected density with the velocity dispersion:

$$\Sigma(R) = \sigma_{LOS}^2(R) = 2\int_R^\infty \left(1-\beta(z)\frac{R^2}{z^2}\right)\frac{\nu(r)\sigma_r^2(r)}{\sqrt{r^2-R^2}}dz$$

Which are called *Equations of projected σ-profile*

...

Therefore the mass density $\rho(r)$ is proportional to the number density $\nu(r)$:

$$\rho(r) \propto \nu(r) \qquad \Rightarrow \quad \text{mass follows light}$$

This is valid also dor galaxies in a cluster

...

The problem of the jeans equation is that we need to know a lot of data which is complex to obtain.

The tensorial Virial Theorem

$$\int \text{Boltz. eq.} \times v_j d^3\bar{v}$$

...

$$\underbrace{\int x_k \frac{\partial \rho \bar{v}_j}{\partial t} d^3\bar{x}}_{A} = \underbrace{-\int x_k \frac{\partial(\rho v_i \bar{v}_j)}{\partial x_i} d^3\bar{x}}_{B \quad \to 2k_{jk}} = \underbrace{-\int \rho x_k \frac{\partial \Phi}{\partial x_j} d^3\bar{x}}_{C \quad \text{comp. } W_{jk}}$$

$$I_{jk} = \int \rho x_j x_k d^3\bar{x}$$

$$K_{jk} = T_{jk} + \frac{1}{2}\Pi_{jk}$$

where T_{jk} is the streaming matrix and Π_{jk} is the radiatio matrix.

...

$$\frac{1}{2}\frac{d^2 I_{jk}}{dt^2} = 2T_{jk} + W_{jk}\Pi_{jk} + W_{jk}$$

4.78 -> steady state:

$$0 = 2k_{jk} + W_{jk} \qquad trace \qquad 0 = 2k + W$$

…

Pros:

integral quantities easier to measure

β does not compear in the equations

Cons:

test part. give the total mass

Generalized Virial Theorem

$$n\frac{d\Phi}{dt} = n\frac{GM(r)}{r^2} = -\frac{d(n\sigma_2^r)}{dr} - \frac{2n}{r}(\sigma_r^2 - \sigma_\tau^2)$$

If we integrate from 0 to ∞ and multiply for $4\pi r^3 dr$ we get:

$$\int_0^\infty n\frac{d\Phi}{dt}4\pi r^3 dr = \int_0^\infty -\frac{d(n\sigma_2^r)}{dr}4\pi r^3 dr - \int_0^\infty \frac{2n}{r}(\sigma_r^2 - \sigma_\tau^2)4\pi r^3 dr$$

$$-|n\sigma_2^r 4\pi r^3|_0^\infty + \int_0^\infty n\sigma_2^r 12\pi r^2 dr - \int_0^\infty 2n(...)4\pi r^2 dr$$

…

$$\int_0^\infty n\frac{d\Phi}{dr}4\pi r^2 dr = \int 4\pi r^2 n(-2\sigma_r^2 + 2\sigma_\tau^2 + 3\sigma_r^2)dr$$

$$\frac{\int_0^\infty nr\frac{d\Phi}{dr}4\pi r^2 dr}{\int_0^\infty n4\pi r^2 dr} = \frac{\int_0^\infty \sigma^2 n4\pi r^2 dr}{\int_0^\infty n4\pi r^2 dr}$$

$$\langle 2\frac{d\Phi}{dr}\rangle = \langle \sigma^2 \rangle$$

$$\frac{d\Phi}{dr} = \frac{GM(r)}{r^2} = -\frac{GM_\infty F(r)}{r^2}$$

$$F(r) = \frac{M(r)}{M_\infty} \leq 1$$

$$\langle r\frac{d\Phi}{dr}\rangle = \langle \sigma^2 \rangle = \langle G\frac{M_\infty F(r)}{r^2}\rangle$$

$$GM_\infty = \frac{\langle \sigma^2 \rangle}{\langle r^{-1} F(r) \rangle}$$

mass follows light:

$$\frac{3\pi}{2} \langle \sigma^2_{LOS} \rangle R_{VT}$$

…

Carberg

TODO: add plots from the red notebook

$$b = \left(\frac{M^{(}_{J.eq}2)}{L}(r) \cdot \frac{L_{tot}}{M_{VT}} \right)$$

$$M_j \to M_{150} \to M(<r) = 3\frac{\beta_{fit,gal}}{G}$$

$$M(r_{max}) = M_{VT} \Bigg(1 - \underbrace{\frac{4\pi r^3_{max} n(r_{max})}{\int_0^\infty 4\pi r^2 n(r) dr} \cdot \frac{\sigma^2_r(r_{max})}{\langle \sigma^2 \rangle}_{r_{max}}}_{20\%} \Bigg)$$

to make a sense between the observational and the theoretical equations, we must correct the mass for the 20% of the mass that is not included in the Jeans equation.

typical $\beta \sim 0$

$$\frac{M(r_{max})}{M_{VT}} \sim 0.8$$

Relating Observational and Theoretical Mass Estimates

We may approach the problem from two complementary perspectives:

1. **Jeans equations**: This method is more closely tied to observational data, providing a way to directly infer mass and dynamical properties of a system from measured kinematics and surface brightness.
2. **Modeling the density profile**: Alternatively, we can propose a functional form for the density $\rho(r)$ (or for some underlying function f) and integrate or fit this model to the data, allowing for theoretical exploration of different mass distributions.

Let's consider the Jeams Theorems and a spherical system.

integral motion of a given Φ.

$$I[\bar{x}(t_1), \bar{v}(t_1)] = I[\bar{x}(t_2), \bar{v}(t_2)]$$

Let's suppose f to be the solution of the Boltzmann equation (steady state). This solution is also the solution of the integral of motion.

$$f \iff f = f(I(\bar{x}, \bar{v}))$$

in a spherical potential, we have f to depend on the energy E and the angular momentum $\vec{L}$:

$$f = f(E, \vec{L})$$

if the system is spherical in any other quantity, it depends on the module of the angular momentum:

$$f = f(E, L)$$

…
Poisson equation:

$$\nabla^2\Phi = 4\pi G\rho = 4\pi G \int_V f d^3\bar{v}$$

spherical symmetry:

$$\frac{1}{r^2}\frac{d}{dr}\left(\frac{d\Phi}{dr}\right) = 4\pi G\rho \int f\left(\frac{1}{2}v^2 + \Phi, |\bar{x}\times\bar{v}|\right)$$

relative potential:

$$\Psi = -\Phi + \Phi_0$$

relative energy:

$$\varepsilon = -E + \Phi_0 = \Psi - \frac{1}{2}v^2$$

isotropic dispension tensor $\bar{\sigma}$:

$$f = f(\varepsilon)$$

politropes and Plummer models

We have seen Plummer models for galaxy clusters and polytropes for gas ($p = kp^\gamma$).
...

$$f(\varepsilon) = \begin{cases} F\varepsilon^{n-\frac{3}{2}} & \varepsilon > 0 \\ 0 & \varepsilon \leq 0 \end{cases}$$

$$\rho = \int f ... = c_n\Psi^n \quad \Psi > 0$$

where $n > \frac{1}{2}$ is a finite number.
So we obtain the equation of stellar politropy:

$$\rho = c_n\Psi^n$$

Poisson euation:

$$\frac{1}{r^2}\frac{d}{dr}\left(r^2\frac{d\Psi}{dr}\right) + 4\pi G c_n\Psi^n = 0$$

$$s = \frac{r}{b}, \qquad \psi = \frac{\Psi}{\Psi_0}$$

Lane-Emden equation:

$$\frac{1}{s^2}\frac{d}{ds}\left(s^2\frac{d\psi}{ds}\right)=\begin{cases}-\psi^n & \text{for } \psi>0\\ 0 & \text{for } \psi\le 0\end{cases}$$

$$\psi=\frac{1}{\sqrt{1+\frac{1}{3}s^2}}$$

we have a special case for $n=5$ (Globular clusters):

$$\rho=c_5\Psi^5=\frac{c_5\Psi_0^5}{\left(1+\frac{1}{3}s^2\right)^{5/2}}$$

therefore, for big radius we have the density *rho* to behave as r^{-5}
another important case is $n\to\infty$
…
Euler equation:

$$\cancel{\text{vel. field}}\quad \underbrace{-\frac{1}{\rho}\frac{dp}{dr}-\frac{d\Phi}{dr}}_{\text{hydrostatic eq.}}=0$$

$$\frac{dp}{dr}=-\rho\frac{d\Phi}{dr}$$

$$k\gamma\rho^{\gamma-1}\frac{d\rho}{dr}=-\rho\frac{d\Psi}{dr}$$

let's multiply for ρ^{-1}:

$$k\gamma\rho^{\gamma-2}\frac{d\rho}{dr}=-\frac{d\Psi}{dr}$$

$$\int_0^{\rho}(\rho')^{\gamma-2}d\rho'=-\frac{1}{k\gamma}\int_0^{\Psi}d\Psi'$$

We have:

$$\frac{1}{\gamma-1}=n\qquad\xrightarrow{n\to\infty}\qquad\gamma\to 1$$

for $n>\frac{1}{2}$ we have $\gamma<3$
…
The Poisson equation for a isothermal gas:

$$\frac{d}{dr}\left(r^2\frac{d\ln\rho}{dr}\right)=-\frac{Gm}{k_BT}4\pi r^2\rho$$

…

Stellar system

$$f(\varepsilon) = \frac{\rho_1}{(2\pi\sigma^2)^{\frac{3}{2}}} \exp\left(\frac{\varepsilon}{\sigma^2}\right) = \frac{\rho_1}{(2\pi\sigma^2)^{\frac{3}{2}}} \exp\left(\frac{\Psi - \frac{1}{2}v^2}{\sigma^2}\right)$$

Therefore:

$$\rho = \int f(\varepsilon) d^3\bar{v} = ... = \rho_1 e^{\frac{\Psi}{\sigma^2}}$$

$$\frac{d}{dr}\left(r^2 \frac{d\ln\rho}{dr}\right) = -\frac{4\pi G}{\sigma^2}\rho$$

there is a relation between the temperature and the dispersion velocity:

$$\sigma^2 = \frac{k_B T}{\mu}$$

$$\bar{v}^2 = \frac{\int v^2 f d^3\bar{v}}{\int f d^3\bar{v}} = 3\sigma^2$$

$$\rho = \frac{\sigma^2}{2\pi G} r^{-2}$$

for a singular isothermal sphere:

$$\rho \xrightarrow{r\to 0} \infty, \qquad M \xrightarrow{r\to\infty} \infty$$

We have a problem:

$$\rho \xrightarrow{r\to 0} \infty$$

therefore, we need to normalize the density:

$$\tilde{\rho} \equiv \frac{\rho}{\rho_0}$$

where $\rho_0 = \rho(r=0)$

$$\tilde{r} = \frac{r}{r_0}, \qquad where \qquad r_0 = \sqrt{\frac{9\sigma^2}{4\pi G\rho_0}}$$

Therefore:

$$\Sigma(r_0) = \frac{1}{2}\Sigma(R=0)$$

...
Another problem is that $M \xrightarrow{r\to\infty} \infty$:

$$f_k(\varepsilon) = \begin{cases} \rho_1 (2\pi\sigma^2)^{\frac{3}{2}} \left(e^{\frac{\varepsilon}{\sigma^2}} - 1\right) & \varepsilon > 0 \\ 0 & \varepsilon \le 0 \end{cases}$$

Which is the king model.

Bibliography

[1] Eva K. Grebel. *Dwarf Galaxies in the Local Group and in the Local Volume*. 2001. arXiv: astro-ph/0107208 [astro-ph]. URL: https://arxiv.org/abs/astro-ph/0107208.

[2] Hannu Karttunen et al. *Fundamental astronomy*. English. 5th ed. United States: Springer, 2007.

[3] Peter Schneider. *Extragalactic Astronomy and Cosmology: An Introduction*. Springer Berlin Heidelberg, 2015. ISBN: 9783642540837. DOI: 10.1007/978-3-642-54083-7. URL: http://dx.doi.org/10.1007/978-3-642-54083-7.